



**CHALMERS**  
UNIVERSITY OF TECHNOLOGY



# FOWT Hybrid Substructure Analyses

A comparison between Orcaflex and Sima software  
Master's thesis in Naval Architecture and Ocean Engineering

GENCO BARIŞ ATALAY

DEPARTMENT OF MECHANICS AND MARITIME SCIENCES  
CHALMERS UNIVERSITY OF TECHNOLOGY

Gothenburg, Sweden 2022  
[www.chalmers.se](http://www.chalmers.se)



MASTER'S THESIS IN NAVAL ARCHITECTURE AND OCEAN  
ENGINEERING

# **FOWT Hybrid Substructure Analyses**

A comparison between Orcaflex and Sima software

Genco Barış Atalay

Department of Mechanics and Maritime Sciences  
*Division of Marine Technology*  
Gothenburg, Sweden  
CHALMERS UNIVERSITY OF TECHNOLOGY  
Gothenburg, Sweden 2022

FOWT Hybrid Substructure Analyses  
A comparison between Orcaflex and Sima software  
Genco Barış Atalay

© Genco Barış Atalay, 2022-05-23

Supervisors at the company: Yungang Liu, Frederik Arvidsson  
Examiner: Wengang Mao, Mechanics and Maritime Sciences  
Supervisor at Chalmers: Wengang Mao, Mechanics and Maritime Sciences

Master's Thesis 2022:72  
Department of Mechanics and Maritime Sciences  
Division of Marine Technology  
Gothenburg, Sweden  
Chalmers University of Technology  
SE-412 96 Gothenburg  
Sweden  
Telephone: + 46 (0)31-772 1000

Cover: Semi-submersible floater type Floating Offshore Wind Turbine

Department of Mechanics and Maritime Sciences  
Gothenburg, Sweden 2022-05-23

FOWT Hybrid Substructure Analyses  
A comparison between Orcaflex and Sima software  
Master's thesis in Naval Architecture and Ocean Engineering  
Genco Barış Atalay  
Department of Mechanics and Maritime Sciences  
Division of Marine Technology  
Gothenburg, Sweden  
Chalmers University of Technology

The usage of SESAM modules to estimate the responses of a hybrid substructure from a given set of boundary conditions. The substructure model which was given by Bassoe Technology will be analyzed. Initially three models are presented, the Panel Model, Morison Model and Mass Model. The Panel Model gives physical information about the Substructure (i.e., displaced volume, shape, etc....). The Morison Model incorporates the second order wave loads on a structure which come from drag and inertial effects such as viscous effects or turbulence. The Mass Model gives data about the mass of each individual element. When these models are introduced to SESAM environment, taken as FEM files and ran on GeniE to be able to be imported into other models. The WADAM wizard in Hydro-D must be run to get the required data so that an analysis in Sima can be done. The WADAM will be using predefined environmental data and the panel, model, and mass models. The WADAM will output all the Kinetics and GDF Geometry required in Sima. Sima will be run to get the non-linear motions and station keeping analysis. The same analysis was run in ORCAFLEX with generated wind data using Turbosim. The ORCAFLEX and Sima carry out the same simulation with different types of inputs. These simulations are carried out to understand the mooring system stresses forces as well as WASIM export to understand the sectional loads. The Sima simulation uses a uniform wind model while ORCAFLEX uses generated values. At the end of these simulations, the results are compared to analyze the methodology used.

## **Preface**

Firstly, I would like to thank the people from Bassoe Technology for their support during the project. Their help with the project and supervision by Mr. Mao has been extraordinary.

In this study, all the results have been taken from computer simulations. The methodology used takes place from February 2022 until May 2022. The work is a part of a research project concerning the static and dynamic responses of a semi-submersible substructure. The project is carried out remotely, with online participants from Bassoe Technology and the Department of Mechanics and Maritime Sciences.

This project was carried out with Genco Atalay as a researcher, Wengang Mao, Frederik Arvidsson and Yungang Liu as supervisors.

Göteborg March 2022-05-23

Genco Barış Atalay

# Contents

Preface.....	II
Contents .....	III
List of Tables .....	V
List of Figures .....	VI
Abbreviations.....	VII
1 Introduction.....	1
1.1 Background .....	1
1.2 Objectives.....	2
1.3 Thesis Structure.....	2
1.4 Scope and Limitations.....	3
2 Literature Review.....	5
2.1 Offshore Platform Type .....	5
2.2 Approach .....	5
2.3 Environmental Loads .....	6
2.3.1 Waves.....	6
2.3.2 Wind.....	7
2.3.3 Current .....	7
2.3.4 Coupling of Environmental Effects .....	7
2.4 Available Software .....	8
2.5 Choice of Software Modules.....	8
2.5.1 GeniE .....	10
2.5.2 Hydro-D .....	10
2.5.3 Using Hydro-D Output .....	12
2.5.4 Sima .....	12
3 Methodology .....	13
3.1 Coordinate System .....	13
3.2 Body Motion Terminology.....	13
3.3 Wind.....	14
3.4 Wave.....	15
3.4.1 Wave Drag Forces.....	16
3.4.2 Linear Potential Model .....	16
3.5 Current.....	18
3.6 Force Models.....	18
3.6.1 Convolution Integral .....	21

3.6.2	Separation of Motions.....	21
3.7	Anchor lines (Catenary System) .....	22
3.8	Equations of motion .....	23
3.9	Positioning.....	24
4	Simulation Procedure.....	25
4.1	Sesam Manager .....	25
4.2	GeniE.....	25
4.3	Hydro-D .....	26
4.3.1	Wadam Analysis Creation .....	26
4.3.2	Wadam Analysis Execution .....	30
4.3.3	Wadam Analysis Results .....	31
4.4	Sima.....	31
4.4.1	Simulation Choice.....	32
4.4.2	Simo Task Location .....	32
4.4.3	Simo Body Creation.....	32
4.4.4	Catenary System .....	32
4.4.5	Slender Elements .....	34
4.4.6	The RNA.....	35
4.4.7	Environment Specifications .....	36
4.4.8	The Simulation.....	37
5	Results.....	38
5.1	0 Degree Direction .....	41
5.2	30 Degree Direction .....	43
5.3	60 Degree Direction .....	45
6	Comparison between Sima and Orcaflex.....	47
7	Conclusion and Future Work .....	50
8	References.....	51
9	Appendix A: Software Images.....	54



## List of Tables

<b>Table 2.1:</b> Drag Coefficients .....	7
<b>Table 2.2:</b> Current Specifications.....	7
<b>Table 4.1:</b> Wave Period Settings .....	27
<b>Table 4.2:</b> Location Variables and Values .....	28
<b>Table 4.3:</b> Coordinate System Specifications .....	29
<b>Table 4.4:</b> Loading Condition Specifications .....	30
<b>Table 4.5:</b> Catenary System Input Table .....	32
<b>Table 4.6:</b> Mooring Line Segments.....	33
<b>Table 4.7:</b> Segmented Line Type Specifications .....	33
<b>Table 4.8:</b> Attachment Point Specifications.....	34
<b>Table 4.9:</b> Tower Cross Section Specifications .....	34
<b>Table 4.10:</b> Simo Tower Configuration .....	35
<b>Table 4.11:</b> Wind Wave Configuration .....	36
<b>Table 4.12:</b> Swell Wave Configuration.....	36
<b>Table 4.13:</b> Wind Configuration .....	36
<b>Table 4.14:</b> Current Configuration.....	36
<b>Table 6.1:</b> Comparison of Results in the 0 Degree Weather Direction.....	47
<b>Table 6.2:</b> Comparison of Results in the 30 Degree Weather Direction.....	48
<b>Table 6.3:</b> Comparison of Results in the 60 Degree Weather Direction.....	48

## List of Figures

<b>Figure 2.1:</b> FOWT Platform Types (Meysam, et al., 2017).....	5
<b>Figure 2.2:</b> Generated Wave Data.....	6
<b>Figure 2.3:</b> Model T2 in GeniE.....	9
<b>Figure 3.1:</b> Coordinate System Definition.....	13
<b>Figure 3.2:</b> Interpolated Current Profile .....	18
<b>Figure 3.3:</b> Dynamic Tension Computation Model .....	22
<b>Figure 4.1:</b> GeniE Flowchart .....	26
<b>Figure 4.2:</b> FOWT Facing Direction.....	27
<b>Figure 4.3:</b> Hydro-D Flowchart .....	31
<b>Figure 4.4:</b> Sima Flowchart .....	37
<b>Figure 5.1:</b> Movement Directions (Hermenau, 2013).....	38
<b>Figure 5.2:</b> Wind Profile .....	38
<b>Figure 5.3:</b> Current Profile.....	39
<b>Figure 5.4:</b> Wave Elevation .....	39
<b>Figure 5.5:</b> Wave Elevation between 20 and 60 seconds .....	39
<b>Figure 5.6:</b> Quasi-static Axial Force at Element 4.....	40
<b>Figure 5.7:</b> Quasi-static Axial Force at Element 1.....	40
<b>Figure 5.8:</b> Total Force in the X Direction .....	40
<b>Figure 5.9:</b> Change in X direction 0 Degrees .....	41
<b>Figure 5.10:</b> Change in Y direction 0 Degrees .....	41
<b>Figure 5.11:</b> Change in Z direction 0 Degrees.....	41
<b>Figure 5.12:</b> Change in Roll 0 Degrees.....	42
<b>Figure 5.13:</b> Change in Pitch 0 Degrees .....	42
<b>Figure 5.14:</b> Change in Yaw 0 Degrees.....	42
<b>Figure 5.15:</b> Change in X direction 30 Degrees .....	43
<b>Figure 5.16:</b> Change in Y direction 30 Degrees .....	43
<b>Figure 5.17:</b> Change in Z direction 30 Degrees.....	43
<b>Figure 5.18:</b> Change in Roll 30 Degrees.....	44
<b>Figure 5.19:</b> Change in Pitch 30 Degrees .....	44
<b>Figure 5.20:</b> Change in Yaw 30 Degrees.....	44
<b>Figure 5.21:</b> Change in X direction 60 Degrees .....	45
<b>Figure 5.22:</b> Change in Y direction 60 Degrees .....	45
<b>Figure 5.23:</b> Change in Z direction 60 Degrees.....	45
<b>Figure 5.24:</b> Change in Roll 60 Degrees.....	46
<b>Figure 5.25:</b> Change in Pitch 60 Degrees .....	46
<b>Figure 5.26:</b> Change in Yaw 60 Degrees.....	46
<b>Figure 9.1:</b> T1 model in GeniE .....	54
<b>Figure 9.2:</b> T2 model in GeniE .....	54
<b>Figure 9.3:</b> T5 model in GeniE .....	55
<b>Figure 9.4:</b> Hydro-D Model Composite.....	55
<b>Figure 9.5:</b> Xtract Pressure view from 0 Deg Weather Direction .....	56
<b>Figure 9.6:</b> Wadam Analysis Pressure Distribution.....	56
<b>Figure 9.7:</b> Riflex Tower (left) and Simo Tower (right).....	57
<b>Figure 9.8:</b> Sima Cylinder RNA .....	57
<b>Figure 9.9:</b> Simo Hub.....	58

## Abbreviations

CAPEX	Capital Expenditure
DNV	Det Norske Veritas
DNV GL	Det Norske Veritas Germanischer Lloyd
FE	Finite Element
FEA	Finite Element Analysis
FEM	Finite Element Model
FOWT	Floating Offshore Wind Turbine
FWT	Floating Wind Turbine
RNA	Rotor-Nacelle-Assembly
OPEX	Operating Expenditure
TLP	Tension Leg Platform
SESAM	Strength Assessment of Offshore Structures
SIF	Standard Interchange Format
SPAR	Named after navigation channels, it is a type of substructure for floating offshore wind turbines
WT	Water Line
XG	Global Coordinate System
XR	Body-relative Coordinate System



# 1 Introduction

## 1.1 Background

The world as we know it is moving towards a more sustainable future. As the world's population increases, so do our energy needs. To achieve the goal of having a sustainable future with an acceptable production/consumption ratio, it is important to have renewable energy alternatives. One of the major alternatives is wind energy.

To meet the increasing need for zero-emission renewable energy demands, novel energy technologies are essential. With vast wind resources that are available in deep water areas, the Floating Offshore Wind Turbine (FOWT) is a great alternative to utilize the wind energy (Ojo, et al., 2022).

From ancient Babylon to the polders of Netherlands, wind energy is and has been in use for millennia. The utilization of the mechanical energy provided by the turning of blades via wind has been a staple of energy for many years. At this point in history, we use it to provide electrical energy to power our towns, cities, and civilization.

To utilize the power of wind, the area where the installation of wind turbine must have good wind intake, low price for lease/purchase, available for high noise production and with lower turbulence. Other important aspects that should be considered are the environmental factors, such as temperature, humidity, corrosive properties, depth of the marine environment, marine growth, accessibility via sea/land/air, etc....

As the energy we harvest from offshore wind sources increase, the individual energy capacity of each wind turbine is gradually increased to greater proportions (Li, 2022). It is important to note that as the population increases, the increase is exponential. Thus, this exponential growth in population procs an exponential growth in the requirement of energy as the required energy to sustain a person has been increasing over the years. To overcome this exponentially increasing demand for energy any alternative to fossil fuels must be continually increasing in efficiency while reducing in cost. One of the major challenges present is to utilize the incredible potential of wind sources in deep water zones. The current offshore wind energy is mostly supplied from bottom-fixed wind turbines which require shallow water installation. Since wind energy is a key creator to today's carbon-free energy supply, it is imperative to design the floater at minimum cost to be able to unlock the fully economically feasible potential of offshore deep water wind farms (Pegalajar-Jurado, et al., 2022). For this increase in cost-efficiency to happen, engineers must be able to fit the requirements with the highest precision possible. This is an important aspect as many of the problems and inputs that are present in the problem definition of a floating offshore wind turbine are stochastic in nature.

Floating offshore wind turbines are an excellent option in our growing world as the more installations are made, surface of land that we use does not reduce. This is exceptionally important as onshore installments of wind turbines are more costly in the long run as they also reduce the amount of land used.

Thus, for all these reasons, it is imperative to create the most cost-efficient version of the offshore wind turbine to allow a truly sustainable future.

## 1.2 Objectives

This thesis will examine the hydrodynamic responses of a given substructure of a floating offshore wind turbine, which later will be simulated in a time-domain procedure. Specific responses will be required, and results will be compared with other time-domain simulations of the same substructure to verify the results presented from the simulations.

The reason why we employ hydrodynamic response analysis is that: companies prepare in advance their plans for FOWT installments. Planning in advance requires a successful simulation of the environment and structure which allows for the company to estimate the usefulness of their product. Currently, a large amount of time has been invested in developing of the systems and tools which will provide insight into the aerohydrodynamic responses of coupled wind turbines to floater structures. However, the speed at which FOWT's are commercially used has been less than expected. As with any newer technology entering the market, the technology is required to be largely tested for different circumstances and the application must be demonstrated to be able to establish credibility (Sethuraman & Venugopal, 2013). A FOWT is used to gain energy from wind sources, since the vessel is in water, there will be a complex system of interaction between the vessel and environment. A simulation of the vessel in the given environment will allow for the optimization of the vessel for any given CAPEX and OPEX calculation.

By understanding the hydrodynamic and aerodynamic response, the engineers can also understand the positioning and mooring line stress that occurs within the system at any given weather condition. Since no company would want to lose their investment, understanding the stresses on the mooring line is crucial. A FOWT experiences many weather conditions during its lifetime, however, the most problematic experiences will be in heavy weather conditions. The FOWT must be built to withstand the destructive wind & wave motions that occur during those heavy weather conditions. By simulating them in software, the company can revise/optimize the vessel design.

Thus, the aim of this research is to simulate the FOWT in software and retrieve relevant data and cross-check if the results are viable.

## 1.3 Thesis Structure

- **Chapter 1:** General introduction into the project. Includes the background information and the objectives of the project with scope and limitations of the project.
- **Chapter 2:** Literature review of the thesis. A review of the environmental effects and the reasoning behind the coupling of these forces. A debate about available software. Includes the SESAM (Software for hydrodynamic and structural analysis of renewable, offshore, and maritime structures.) package overview with all the given modules and their respective uses with discussion of importance to the project in general. The modules are explained in depth.

- **Chapter 3:** The methodology that will be used as well as the theoretical background of the process will be explained.
- **Chapter 4:** The simulation process which is being used to reach the results of the thesis is explained step-by-step and in detail. This chapter will be the main process of the thesis.
- **Chapter 5:** The results will be presented in this part of the thesis. The results of all steps will not be added, only the relevant results from the Sima simulation (Hydrodynamic response) will be reported.
- **Chapter 6:** Comparison of results from Sima (Simulation and analysis for marine operations and floating systems) and Orcaflex (A software that performs global static and dynamic analysis of a wide range of offshore systems, typically including boundary conditions such as vessels, buoys, etc., as well as finite element modelling of line structures.) will be conducted in this part. This will set the stage for the next chapter as it discusses the validity of the previous steps.
- **Chapter 7:** The conclusion of the thesis will be presented. Future work and possible further investigations will be discussed in this chapter.
- **Chapter 8:** The references pertaining to the thesis will be listed.
- **Chapter 9:** Appendix A where figures relating to the thesis procedure will be displayed.

## 1.4 Scope and Limitations

To be able to simulate the substructure in for various realizations, a detailed time window must be constructed. The simulations must be long enough to create a visualization of the substructure in question. Since the model will be subjected to a time-domain simulation, the simulation timestep and length must be optimized. Different visualizations must be viewed to understand the nature of the substructure. The mean of the parameters as well as the standard deviations of these parameters are considered. However, these parameters must be limited to realistic conditions that represent the most realistic outcome. These parameters can't be infinite as well, specific ones must be chosen to be good indicators. The following are some explanations into the limitation of usage in the software modules that will be later discussed in Chapter 2 and 4. The reasoning behind some of the choices in these chapters can be found below as they are reflected upon here to show the limitations pertaining to the thesis.

- The drag force coefficients are selected from given resources, so to match the different shapes that are part of the model, the drag force coefficients are estimated.
- Hydro-D is explained as a software that can calculate the wave load & stability analysis of fixed and floating structures (DNVGL, 2022). The direction set for the model is used at 45-degree intervals from 0 to 360 for computing

hydrodynamical properties. This is the recommended setting in Hydro-D. It is also possible to set this to 1-degree intervals, however this creates a heavy impact on computational power. The 45-degree interval also computes the values from 0 to 360 degrees. However, it uses 45-degree intervals to extrapolate the values that are required in between the intervals. The hydro model boundary type is set to floating as the model is supposed to be float. Since there are mooring lines attached to the vessel some intermittent type of boundary type is called into question. Since there are only three modes of boundary type description; floating, fixed and specified free modes, the floating model is best suited for our needs. The load from the waves & wind are transferred upon the actual panel model instead of a simplified Morison (beam) model. The actual change of loads on the specific panels is very important to measure as this analysis is required to get the required results for adequate comparison. The Morison load type also requires the model to be either a super element of the panel model or part of it. Weather directions are an important aspect. As the weather direction is set to a certain degree, the wind, wave, and current are set to the same degree. This of course is not the exact same case where all weather effects are aligned perfectly, however it is a simplification that must be made to solve the problem.

- The wind for the Orcaflex was generated in Turbosim (A software that is a stochastic, full-field, turbulent-wind simulator. It numerically simulates a time series of three-dimensional wind velocity vectors at points in a vertical rectangular grid.). The wind value for Sima was used as stationary uniform due to conflict with the input file type from Turbosim. The mean values of wind were calculated from the generated values from Turbosim.
- The simulation timestep is set to 0.05 seconds are done for 3600 seconds. The reason for the 3600 seconds is to be able to compare the values from Sima to the results from Orcaflex. It is also important to note that 3600 seconds is enough time to visualize the results gathered from the motion of the turbine.
- Wave values are generated, and Sima also incorporates irregular movements within the waves.



## 2 Literature Review

### 2.1 Offshore Platform Type

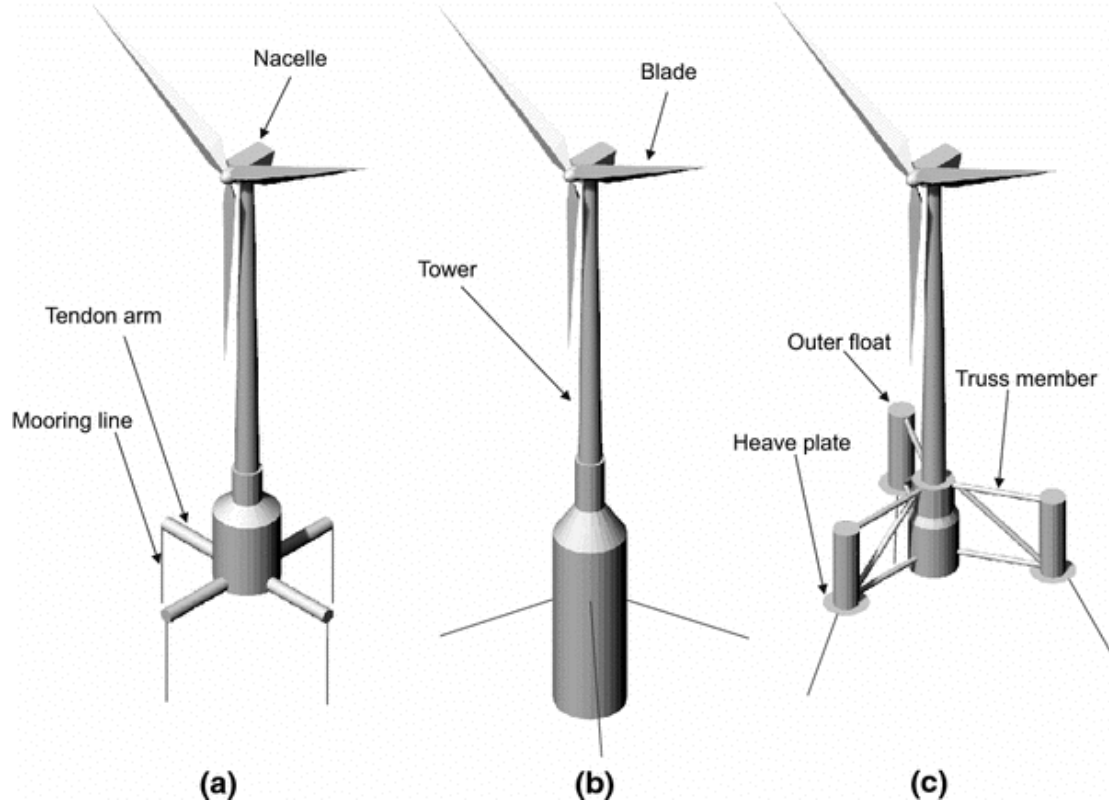


**Figure 2.1:** FOWT Platform Types (Meysam, et al., 2017)

There are three main types of floaters that are used for floating offshore wind turbines: tension leg platforms (TLP's), SPAR and semi-submersibles. In the figure above, (a) represents tension leg platforms, (b) is the SPAR platform and (c) is the semi-submersible platform (Meysam, et al., 2017).

The three types differ in stabilization methods. The TLP is stabilized using the mooring lines with high tension values which act on the lines. The SPAR platform is stabilized with the ballast within the main body and the semi-submersible is stabilized with the buoyancy which acts upon the vessel.

Although all three types of platforms have mooring lines, their influences on the stabilization of the platforms differ. TLP's usually having the highest stabilization, however, have the highest tension on the mooring lines and anchoring systems.

While the semi-submersible will use the platforms' own properties to stabilize and only have catenary mooring lines to anchor the platform. The semi-submersible type will be used.

### 2.2 Approach

The research investment pertaining to offshore wind turbines should be focused around calculating the effects of coupled wind wave and current effects since the FOWT has a complex multi-degree of freedom coupling system. The very environment the FOWT

is situated is subjected to constant change (Wang, et al., 2022). Since the FOWT will be in marine environment with coupled wind wave and current effects, there is a need to define these environmental effects as well as choose software that can provide required simulations.

## 2.3 Environmental Loads

All structures are subject to environmental loads. This is especially important to distinguish in a FOWT since the structure itself is afloat on a body of liquid which has a current. The combination of all these loads requires a coupled analysis where the environmental effects can be calculated together with dynamic response to truly see the effects. The effects of the environmental loads are applied together to get the dynamic response. The environmental loads are also time dependent i.e., having a different wave face the vessel at different times requires a more in-depth dynamic analysis, with also dynamic irregular wave movements considered.

### 2.3.1 Waves

Sea waves have a tremendous effect on FOWT's as they are one of the three major driving forces that dictate motion and rotation of the vessel. The in-depth theory behind wave kinematics and specifics will later be covered in Chapter 3. The waves that will be applied in the simulation must be generated. This is done because the generated wave values present the possible irregularities in encountered wave faces. Below an example of generated wave values can be viewed.

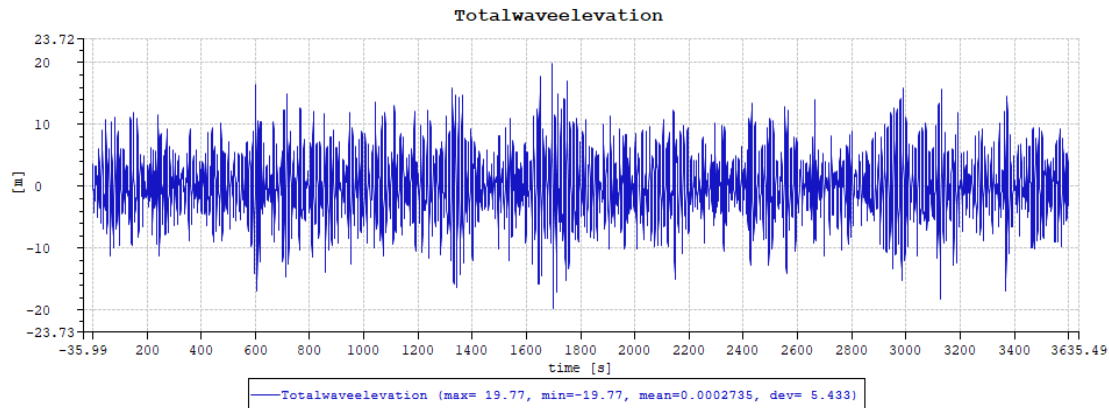


**Figure 2.2:** Generated Wave Data

As is evident from the figure, not all waves have the same wave height, however, follow a similar trend in increase and decrease in significant wave height with respect to time.

#### 2.3.1.1 Wave Drag Forces

The liquid to solid interaction between the waves and the structure causes drag forces that must be considered when calculating the effects of environmental conditions. The physical effect of the surface waves can be thought of the composition of force related to mass and the drag force (Beji, 2020). Thus, by using the Morison equation and the Morison model, one can calculate such wave effects (Orcina, 2022).

### 2.3.2 Wind

The wind is the second greatest influence on the motion and rotation of the FOWT. Wind is a complex structure which can be thought of as the driving force of the blades in the turbine. The wind moves towards the blades and by friction and lift, the blades are turned to create electrical energy. Wind also interfaces with every part of the FOWT which is above the water line. The drag coefficients thus, are very different from parts to parts. A general simplification is required to solve this problem. By using a simplification of external resources, the drag coefficients are selected as:

**Table 2.1:** Drag Coefficients

	Quadratic Longitudinal Drag	Quadratic Transverse Y	Quadratic Transverse Z
Drag coefficient	1.1	0	1.1

This simplification is only done for slender elements above the waterline (attached to the floater body), the main quadratic wind drag coefficients are input as a kinetic property of the floater body. The wind data will be taken as uniform throughout the simulation environment. A more in-depth look at governing wind equations as well as coupling effects will be discussed in Chapter 3.

### 2.3.3 Current

The current itself is a driving force of the sub-water line effects. As there is Morison-like loading that happens below the waterline which influences the movement of the FOWT, it is important to model this effect. The input data is as follows:

**Table 2.2:** Current Specifications

Depth [m]	Uc, ratio [-]	Uc, 1 year [m/s]	Uc, 50 year [m/s]
0	1.00	0.95	1.34
-20	0.88	0.84	1.18
-28	0.81	0.77	1.09
-36	0.78	0.74	1.04
-45	0.74	0.70	0.99
-53	0.73	0.69	0.97
-61	0.71	0.67	0.95
-70	0.67	0.64	0.90
-78	0.64	0.61	0.86
-86	0.62	0.59	0.83
-97	0.53	0.50	0.71
-100	0.00	0.00	0.00

### 2.3.4 Coupling of Environmental Effects

For the evaluation of fatigue life of a FWT, the wind-wave coupling effects must be considered as the responses of the FWT are affected by the resulting interactions between hydrodynamic and aerodynamic loads (Yang, et al., 2020). The fact that there are multiple major environmental forces acting upon the FOWT means that a coupled analysis must be undertaken to provide accurate results. As an initial step, the integrated

coupled dynamics model with the aero-hydrodynamic properties and the multibody dynamics must be incorporated with the finite element (FE) method (Song, et al., 2021). To be able to incorporate any environmental loads into a simulation, one must first create a FEM (Finite Element Model), onto which the environmental effects can be subjected. Bassoe Technology has provided with an FEM model. Which is used as the physical representation of the FOWT (Bi, 2019).

## **2.4 Available Software**

With the goal of coupling environmental effects to be subjected on a 3D body, a deeper search into available software is needed. In industry applications, simulation of the FOWT is done via many methods and software packages. Some examples to the possible software are SESAM, Orcaflex, HAWC2 (Larsen & Hansen, 2015), etc.... These software packages are used to simulate the aero-hydrodynamic reactions of a vessel in marine environments. SESAM can be used to simulate the aero-hydrodynamic responses of floating structures (Beshbichi, et al., 2021). SESAM package has many modules that are integrated with each other to provide results. These results can be from every aspect of the FOWT from the stress on any point of the blades to the axial stress on the mooring lines (DNV, 2022). Orcaflex is a software that can calculate the aero-hydrodynamical responses with mooring line stresses as well (Pillai, et al., 2022). HAWC2 is an aero-hydro-servo-elastic software that can be used to compute the design load for the fully coupled ambient interactions (Wandji, et al., 2016).

The 10 MW floating offshore wind turbine that was used is given by Bassoe Technology. To understand and get the required outputs, software that can perform time-domain simulations is required. The SESAM software package from DNV-GL is chosen to be used to analyze the model.

In the initial part of the thesis planning, a linear regression analysis (Mao, et al., 2015) was discussed. The linear regression analysis was discussed to see if the method was better than FEA. The linear regression method's reliability was to be discussed and portrayed. However, due to time limitations the regression analysis was not explored.

## **2.5 Choice of Software Modules**

A module that can use an FEM file as an input is needed. Furthermore, software that has the capabilities to handle the FEM file and output a FEM file is needed. Also, the program should not change the properties of the FEM file, only provide a readable/usable version of the FEM file for further use. The initial FEM file containing the panel model T2 is given.

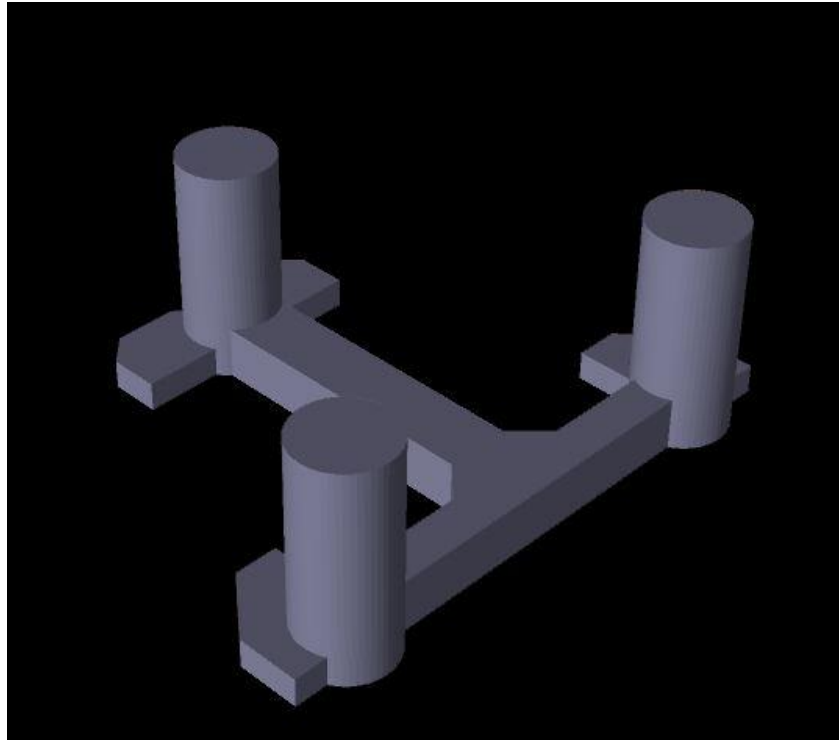


**Figure 2.3:** Model T2 in GeniE

The figure above represents the physical panel model with the parts of the substructure above the water line. To handle the problem a look into SESAM feature description is needed.

From the handbook, the preprocessing main tools are explained in depth. Since our first goal is to get the hydrodynamical properties from Hydro-D which can't read the given FEM format, other preprocessors are investigated.

- **Submod:** Provides a more in-depth look at the local level of a given model.
- **Patran-Pre:** The license for this software was not included in the SESAM package received.
- **Presel:** Only assembles premade models into bigger models, which does not suit our needs.
- **Genie:** GeniE is a very strong tool with many applications including the creation of the model from scratch. This software allows for FEM input and output by only checking the integrity of the FEM file. GeniE, however, is very complex software.

From the strong tools that SESAM provides, GeniE seems to be the best option out of all the choices. GeniE itself is very complex software which allows for many complex alterations and creations, so it is important to understand how to use the software.

### 2.5.1 GeniE

GeniE provides Guiding Geometry options for creating the general structural model. These guiding geometries can be exemplified as: points, lines, polylines, conic sections, free-form curves, split/joint curves, curves on surfaces, planes, point sets, point grids, modelling grids, transformations, and profiles. These elements are used to create the actual concept model which will be used for analysis reasons. The guiding geometries are used solely for the model creation within GeniE (DNVGL, 2022).

After the guiding geometry has been set, the structure itself can be created. This model consists of beams, plates, shells, supports, joints, and masses. From the structural model, an FEM model can be created and stored in the SESAM Input Interface. This model can be later transferred to other SESAM package software for wave load calculation and structural analysis (DNVGL, 2022).

#### 2.5.1.1 Using the GeniE FEM File

Now that there is a physical representation of the FOWT in a 3D environment, this object must be then moved into an environment where coupled wind, wave and current effects can be subjected. In the SESAM package, there is a module: Sima. This module can provide a time-domain fully coupled simulation (Sintef, 2022). However, to be able to do such a simulation, Sima requires some inputs, mainly hydrodynamic coefficients. These hydrodynamic coefficients are calculated from the interaction between solid and waves. There must be an existing GDF geometry and hydrodynamical values as well as environmental data before importing a 3D object. Hydro-D has an analysis named Wadam (DNVGL, 2022). In Hydro-D, the Wadam analysis uses the Morison equation, first-order, and second-order 3D potential theory for the wave load calculations. The analysis is performed in the frequency domain where the incident wave has Airy wave properties (DNV, 2022). Hydro-D can use the built-in analysis to calculate the wave loads and respective hydrodynamic/static values. These values need to be used in a module that can also incorporate any wind effects present. The details of the coupling of wind effects (both theory and application) will be discussed in detail in Chapter 3 and Chapter 4.

### 2.5.2 Hydro-D

Hydro-D will be used to calculate the hydrodynamical properties of the substructure. The Wadam analysis will be used for the purpose of computing the hydrodynamic outputs. These outputs will then later be used in a simulation to couple wind, wave, and current effects. The actual setting up of the values and Wadam analysis is further discussed in Chapter 4. The outputs that can be taken from Hydro-D are:

- 1) **Structural Mass:** The data of the total mass of the structure, the center of gravity, mass moment of inertia about origin in the x, yx, y, zx, zy and z directions.
- 2) **Linear Damping:** The damping of the movement of the vessel is very important to model as this stops the vessel from moving unnaturally and erratically in all six degrees of freedom (Wang, et al., 2021).
- 3) **Hydrostatic Stiffness Data:** This is very important data to have since hydrostatic stiffness describes how the net weight and buoyancy affects the vessel with change

in locations and rotation. The values in this six-by-six matrix can indicate an imbalance (Ullah, et al., 2021).

- 4) **First Order Motion Transfer Function and Wave Force Transfer:** Shows the amplitudes versus wave periods in all six degrees of freedom for every 45-degree interval from 0 to 360 degrees (DNV, 2022).
- 5) **Wave Drift Force:** Is a graph of the mean forces of ambient waves on floating or submerged vessels. One method of calculation of the wave drift force is by using the direct pressure integration method. It is done by integrating the second-order pressure on the body surface (Seo, et al., 2013).
- 6) **Radiation Data:**
  - a) **Frequency Dependent Added Mass:** Data about added mass (i.e., inertia) added to the system due to acceleration or deceleration caused by interaction (Orcina, 2022).
  - b) **Frequency Dependent Damping:** Data about damping caused by the added mass (Pascual & Adhikari, 2008).
  - c) **Retardation Function:**
    - i) **Linear Damping:** Same matrix as the above Linear Damping.
  - d) **Added Mass Zero Frequency:** Added Mass for zero frequency specifications. The methodologies to obtain these values are mostly numerical. The values which are obtained are done through usually by using the frequency domain. The idea is to use the frequency as a variable and test the limit which moves towards zero frequency to solve the added mass problem. This, however, is very taxing to the computation; the method proposed by Ould el Moctar et al. allows a depth-based approach towards understanding and solving the problem (el Moctar, et al., 2022).
  - e) **Added Mass Infinite Frequency:** Added Mass for infinite frequency specifications (Orcina, 2022).

To get the required data, Hydro-D needs to perform a WADAM analysis. The Wadam analysis will be further discussed in Chapter 4.

Hydro – D uses the Panel Model which is specified in GeniE as the main FEM model. The input FEM file is cut at the waterline and if the FEM extends below the seafloor, it is also cut off below the soil line. All the panels on the wet surface must have hydro pressure or wet surface properties (DNVGL, 2022).

A WAMIT.out file will be created that stores all relevant data as well as supplementary other files that will be used to check the validity of the Hydro-D set-up. Further discussion into the nature of the WAMIT.out file will be discussed in Chapter 4.

### **2.5.3 Using Hydro-D Output**

After Hydro-D has given the required values, they will be imported into an environment where wind, wave and current are able to be coupled and have the 3D model imported into the environment. Another aspect to consider is that the module that must house the effects must also be able to construct a mooring system, as well as the tower of the FOWT and the RNA (Rotor-Nacelle-Assembly). Thus, by looking through the SESAM feature description, Sima will be used to simulate the FOWT in the requested environment. Further details about Sima set-up, usage and relative simulation types will be discussed in Chapter 4. The theoretical knowledge that will be used in the determination of the positioning of the FOWT will be discussed in Chapter 3.

### **2.5.4 Sima**

Sima software is the main tool that will be used to get the responses from the model for the problem definition. The software can run dynamic simulations with 3D and 2D graphical representations. The hydrodynamical coefficients are taken from Hydro-D in the form of GDF geometry as well as WAMIT output files which are created from WADAM analysis in Hydro-D. The catenary system, which is a major actor in the analysis, is added to this software as it has the highest capability to deal with the complex system. The software enables the use of either a docking cone mechanism or a slender system connection to integrate the nacelle assembly to the wind calculations of the turbine thus having a great impact on the study. Sima will allow for the thesis to reach its goal of receiving the required outputs from the problem. As an important note, Sima also allows for visualization of results which is very efficient when using to compare with other software.



### 3 Methodology

In this chapter, the theoretical knowledge and applied methods will be discussed in depth. To retrieve relevant data, one must know the interactions and mathematics behind the simulation process (Sintef, 2022).

#### 3.1 Coordinate System

Before applying advanced mathematics on the vessel, one must define the working environment. Since the FOWT is being handled in a system where it is floating, two coordinate systems are considered: the Global Coordinate System (will be referred as XG) and the Body-related Coordinate System (will be referred as XR) (DNV, 2022).

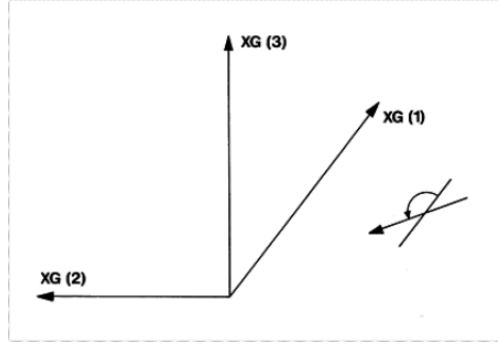


Figure 3.1: Coordinate System Definition

#### 3.2 Body Motion Terminology

Since the FOWT is a body in motion in the water, some specifications/assumptions must be made beforehand.

- Total motion is the motion resulting from all forces acting on the body.
- Wave frequency motion is the motion that results from 1<sup>st</sup> order wave forces.
- Low frequency motion is the motion that results from forces other than the wave frequency: wind, wave drift, current and catenary lines. The wave drift force can be calculated by using the direct pressure integration method:

$$\begin{aligned}
 \overrightarrow{F_{WDF}} = & \frac{1}{2} \rho g \int [\zeta_1 + \zeta_d - - (\xi_3 + \xi_4 Y - \xi_5 X)]^2 \frac{\vec{N}}{\sin \alpha} dl \\
 & - \rho \iint \left[ \frac{1}{2} \nabla(\phi_I + \phi_d) \cdot \nabla(\phi_I + \phi_d) \right] \vec{N} dS \\
 & - \rho \iint [\vec{\xi}_S \cdot \nabla(i\omega(\phi_I + \phi_d)) + H\vec{X} \cdot \nabla gZ] \vec{N} dS \\
 & - \rho \iint [i\omega(\phi_I + \phi_d) - (\vec{U} - \nabla\Phi) \cdot \nabla(\phi_I + \phi_d) \\
 & + g((\xi_3 + \xi_4 Y - \xi_5 X)] \vec{N} dS - \rho \iint [gZ] \vec{N}_2 dS
 \end{aligned} \tag{3.1}$$

The solution of the wave drift force is further explained in “Comparative study on computation of ship added resistance in waves” (Seo, et al., 2013).

- Phase angle:  $\phi_x$ , an angle that is added to the  $\omega t$  term in a transfer function to portray the forward phase shift.
- Transfer function: the relation between harmonic excitation and its linear response:

$$x(t) = R_x \zeta_a (\sin(\omega t + \phi_x)) \quad (3.2)$$

There exists an amplitude ratio of response to excitation of:

$$R_x = \frac{x_a}{\zeta_a} \quad (3.3)$$

- Phase lag:  $\psi_x = -\phi_x$ . The phase lag is the inverse of the phase angle that is used to portray the negative forward phase shift (i.e., the backwards phase shift).

### 3.3 Wind

As mentioned in Chapter 2, the wind shall be taken uniform for the purpose of this assessment. However, with recommendations the ISO 19901-1 Wind spectrum, also referred as the NPD spectrum will be considered since it is recommended with strong winds and simulations that are at most 3600 seconds long. The design wind can be calculated as:

$$u(z, t) = U(z) \left[ 1 - 0.41 \cdot I_u(z) \cdot \ln\left(\frac{t}{t_0}\right) \right] \quad (3.4)$$

The  $U(z)$  is the 1 hour mean wind speed in m/s. It is calculated as

$$U(z) = U_0 \left[ 1 + [5.73 \cdot 10^{-2} (1 + 0.15 \cdot U_0)^{0.5}] \cdot \ln\left(\frac{z}{10}\right) \right] \quad (3.5)$$

The turbulence intensity factor  $I_u(z)$  is

$$I_u(z) = 0.061 + 0.043 \cdot U_0 \left( \frac{z}{10} \right)^{-0.22} \quad (3.6)$$

Where  $U_0$  is the 1 hour mean wind speed at 10 meters (reference height).

The wind force is then calculated as:

$$q_j = C_j(\alpha) v^2 \quad (3.7)$$

Where:

- $j$  is the degree of freedom
- $C$  is the wind force coefficient
- $v$  is the relative wind speed, which uses the speed  $u(z, t)$  and the body speed
- $\alpha$  is the relative velocity direction

### 3.4 Wave

With the given values and implementation recommendations, a JONSWAP spectrum will be deployed to depict the wave movement. To mathematically model the wave, we need the wave spectrum. The wave spectrum is denoted as  $S_{\zeta}^+(\omega)$  and is calculated by:

$$S_{\zeta}^+(\omega) = \left[ \frac{\alpha g^2}{\omega^5} \exp\left(-\beta \left(\frac{\omega_p}{\omega}\right)^4\right) \gamma \right] \exp\left(\frac{\left(\frac{\omega}{\omega_p} - 1\right)^2}{2\sigma^2}\right) \quad (3.8)$$

Where:

- $\alpha$  is the spectral parameter calculated by the significant wave height  $H_s$

$$\alpha = \left( \frac{H_s \omega_p^2}{4g} \right) \frac{1}{0.065\gamma^{0.803} + 0.135} \quad (3.9)$$

- $\omega_p$  is the peak frequency

$$\omega_p = \frac{2\pi}{T_{peak}} \quad (3.10)$$

- $\gamma$  is the peakedness parameter

$$\gamma = \exp\left[3.484 \left(1 - 0.1975\delta \frac{T_p^4}{H_s^2}\right)\right] \quad (3.11)$$

$$\delta = 0.036 - 0.0056 \frac{T_p}{\sqrt{H_s^2}} \quad (3.12)$$

- $\beta$  is the form parameter
- $\sigma$  is the spectral parameter with the values of:  
 $\sigma_a = 0.07$  for  $\omega < \omega_p$   
 $\sigma_b = 0.09$  for  $\omega > \omega_p$

By combining JONSWAP wind sea contribution and JONSWAP swell contribution we achieve:

$$S_{\zeta,TOT}^+(\beta, \omega) = S_{\zeta,1}^+(\omega)\theta_1(\beta - \beta_1) + S_{\zeta,2}^+(\omega)\theta_2(\beta - \beta_2) \quad (3.13)$$

Where:

- $S_{\zeta,1}^+, S_{\zeta,2}^+$  describe power spectra of wave elevation.
- $\theta_1$  and  $\theta_2$  describe wave directions

### 3.4.1 Wave Drag Forces

The Morison Model Provided allows for the understanding of the drag forces as well as the force per length of body to be calculated. The basic Morison equation is used in the calculations:

$$f = C_m \Delta a_f + \frac{1}{2} \rho C_d A |v_f| v_f \quad (3.14)$$

Where:

- $f$  is the fluid force per unit length on the body
- $C_m$  is the inertia coefficient for the body
- $\Delta$  is the mass of fluid displaced by the body
- $a_f$  is the fluid acceleration relative to earth
- $\rho$  is the density of water
- $C_d$  is the drag coefficient for the body
- $A$  is the drag area
- $v_f$  is the fluid velocity relative to earth.

The platform will be oscillating and moving throughout the operation time; thus, the equation must be modified to add the effects of inertia:

$$f = (C_m \Delta a_f - C_a \Delta a_b) + \frac{1}{2} \rho C_d A |v_r| v_r \quad (3.15)$$

Where:

- $C_a$  is the added mass coefficient for the body
- $a_b$  is the body acceleration relative to earth
- $v_r$  is the fluid velocity relative to the body.

Since  $a_r = a_f - a_b$ , this equation will simplify to:

$$f = (\Delta a_f - C_a \Delta a_r) + \frac{1}{2} \rho C_d A |v_r| v_r \quad (3.16)$$

### 3.4.2 Linear Potential Model

The wave field which is used to calculate wave properties such as distributed force, momentum and other properties is defined by using the wave potential  $\Phi_0$ . There are many different waves that occur in real life, these waves income with different frequencies that result in different reactions. Thus, there must be a description of this phenomena that includes the wave amplitude, wave number, wave component phase angle, propagation, and acceleration. Airy's theory allows for the construction and description of such a relationship by:

$$\Phi_0 = \frac{\zeta_a g}{\omega} C_1 \cos(\omega t - kx \cos(\beta) - ky \sin(\beta) + \phi_\zeta) \quad (3.17)$$

Where:

- $\zeta_a$  is the wave amplitude

- $g$  is the gravitational acceleration
- is the wave number

$$\omega^2 = gk \tanh(kd) \quad (3.18)$$

- $\beta$  direction of wave propagation
- $\phi_\zeta$  wave component phase angle
- $C_1$  is a coefficient given by:

$$C_1 = \frac{\cosh(k(z + d))}{\cosh(kd)} \quad (3.19)$$

- $d$  is the water depth

When finite depth of water is concerned,  $C_2$  and  $C_3$  become:

$$C_2 = \frac{\cosh(k(z + d))}{\sinh(kd)} \quad (3.20)$$

$$C_3 = \frac{\sinh(k(z + d))}{\sinh(kd)} \quad (3.21)$$

Particle velocities and accelerations in the undisturbed wave field become:

$$\begin{aligned} v_x &= \zeta_a \omega \cos(\beta) C_2 \sin \alpha \\ v_y &= \zeta_a \omega \sin(\beta) C_2 \sin \alpha \\ v_z &= \zeta_a \omega C_3 \cos \alpha \\ a_x &= \zeta_a \omega^2 \cos(\beta) C_2 \cos \alpha \\ a_y &= \zeta_a \omega^2 \sin(\beta) C_2 \sin \alpha \\ a_z &= -\zeta_a \omega^2 C_3 \sin \alpha \end{aligned} \quad (3.22)$$

$$\alpha = \omega t - kx \cos(\beta) - ky \sin(\beta) + \phi_\zeta \quad (3.23)$$

The surface elevation becomes:

$$\zeta = \zeta_a \sin \alpha \quad (3.24)$$

Linearized dynamic pressure:

$$p_d = \rho g \zeta_a C_1 \sin \alpha \quad (3.25)$$

### 3.5 Current

Since there is an explicitly defined current profile, linear interpolation will be used to create a profile.

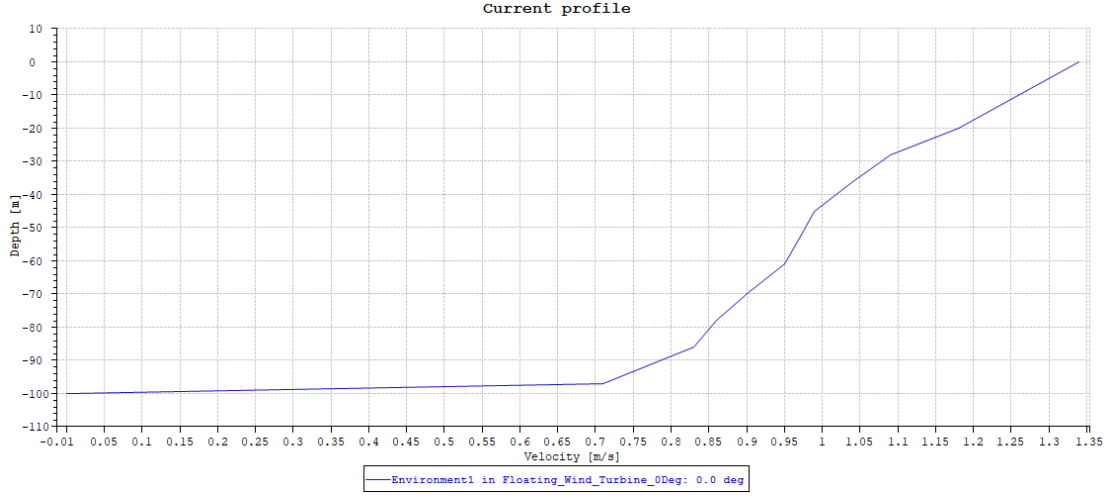


Figure 3.2: Interpolated Current Profile

The current creates current drag forces which is essential to understand the effect of drag on the vessel.

$$q_{CU}(\alpha, t) = C_1(\alpha)|u(t)| + C_2(\alpha)|u(t)|^2 \quad (3.26)$$

Where:

- $C_1$  is the linear current force coefficient
- $C_2$  is the quadratic current force coefficient
- $u$  is the relative velocity
- $\alpha$  is the relative angle difference

### 3.6 Force Models

The force model must allow for the exerted force on the body itself to be represented. To this point we have discussed the properties of the wave and wind structure. However, the direct effect of these forces is not alone enough to depict the exciting force vector. The effects of these forces when coupled with the body create other effects that are used to understand the motion of the vessel. Such effects are the frequency-dependent mass matrix ( $M$ ), body mass matrix ( $m$ ), frequency-dependent added-mass ( $A$ ), frequency-dependent potential damping matrix ( $C$ ), linear damping matrix ( $D_1$ ), quadratic damping matrix ( $D_2$ ), vector function of each element ( $f_i = \dot{x}_i|\dot{x}_i|$ ), hydrostatic stiffness matrix ( $k$ ) and position vector( $x$ ). The relation between these effects must equate to the wind drag force ( $q_{WI}$ ), first order wave excitation force ( $q_{1WA}$ ), second order wave excitation force ( $q_{2WA}$ ), current drag force ( $q_{CU}$ ) and any other forces ( $q_{ext}$ ) such as the coupling drift damping etc... The relationship is the equation:

$$M\ddot{x} + C\dot{x} + D_1\dot{x} + D_2f(\dot{x}) + K(x)x = q(t, x, \dot{x}) \quad (27)$$

$$M = m + A(\omega)$$

$$A(\omega) = A_\infty + \alpha(\omega)$$

$$\begin{aligned}
A_\infty &= A(\omega = \infty) \\
C(\omega) &= C_\infty + c(\omega) \\
C_\infty &= C(\omega = \infty) \equiv 0
\end{aligned}$$

To find the frequency-dependent added mass, one needs to find the radiation force, which requires the radiation potential, which requires an expression of the velocity potential.

$$\phi = \phi_R + \phi_D \quad (3.28)$$

The pressure then can be expressed as:

$$P = \rho g z - \rho \frac{\partial \phi_R}{\partial t} - \rho \frac{\partial \phi_D}{\partial t} \quad (3.29)$$

The radiation force becomes:

$$F^R = -\rho \iint n \frac{\partial \phi_R}{\partial t} dA \quad (3.30)$$

By adding all dimensions of movement and radiation potential, the radiation force becomes:

$$\begin{aligned}
\tau_j^R &= \tau_0^R - \sum_{k=1}^6 a_{jk} \bar{q}_k - \sum_{k=1}^6 b_{jk} \dot{q}_k - \sum_{k=1}^6 c_{jk} q_k \\
&\quad - \sum_{k=1}^6 \int_{-\infty}^t K_{jk}(t - \sigma) \dot{q}_k(\sigma) d\sigma
\end{aligned} \quad (3.31)$$

Where  $a$  is added mass,  $b$  is damping, and  $c$  are the restoration coefficients.  $K_{jk}$  is the impulse response function in direction  $j$  with an impulse that comes from the  $k$  direction.

By adding the sinusoidal frequency  $\omega$ , we can obtain the frequency-dependent added mass as (Wang, et al., 2021):

$$a_{jk}(\omega) = a_{jk} - \frac{1}{\omega} \int_0^\infty K_{jk}(t) \sin \omega t dt \quad (3.32)$$

The damping that is achieved from added mass can be found similarly by using the radiation force equation to obtain:

$$b_{jk}(\omega) = b_{jk} + \int_0^\infty K_{jk}(t) \cos \omega t dt \quad (3.33)$$

After finding the added mass matrix  $A$ , the infinite frequency added mass matrix can be found as:

$$A_i(\infty) = A(f_i) + \frac{1}{2\pi f_i} \int_{s=0}^{T_c} K(s) \sin(2\pi f_i s) ds \quad (3.34)$$

Where  $A$  is the added mass matrix,  $K$  is again the impulse response function,  $f$  is frequency,  $T_c$  is the cut-off time for the impulse response function (Orcina, 2022).

The derivations for the frequency added mass and damping are discussed in “Frequency-Dependent Added Mass in Models for Controller Design for Wave Motion Damping” (Kristiansen & Egeland, 2003).

The Linear Damping and Quadratic Damping coefficients and matrices can be calculated by solving the following formula

$$\ddot{\eta} + (p_1 + p_2|\dot{\eta}|)\dot{\eta} + \omega^2\eta = 0 \quad (3.35)$$

Where:

- $\ddot{\eta}$  is acceleration vector
- $\dot{\eta}$  is velocity vector
- $\eta$  is direction vector
- $p_1$  is the Linear damping coefficient
- $p_2$  is the quadratic damping coefficient

The hydrostatic stiffness can be obtained via (Jonkman, 2010)

$$F_i^{Hydrostatic}(q) = \rho g V_0 \delta_{i3} - C_{ij}^{Hydrostatic} q_j \quad (3.36)$$

Where:

- $F_i^{Hydrostatic}$  is the total hydrostatic load
- $V_0$  is the displaced volume
- $\delta_{i3}$  is the (i, 3) component of the identity matrix
- $C_{ij}^{Hydrostatic}$  is the (i,j) component of the linear hydrostatic-restoring matrix
- $q$  is the degree of freedom

However, since we require a matrix of values the linear hydrostatic stiffness matrix can be given as (Ullah, et al., 2021):

$$k = \begin{bmatrix} 0 & 0 & 0 & 0 & 0 & 0 \\ 0 & 0 & 0 & 0 & 0 & 0 \\ 0 & 0 & \rho g A_0 & 0 & 0 & 0 \\ 0 & 0 & 0 & \rho g \iint y^2 dA + \rho g V_0 r_3^b & 0 & 0 \\ 0 & 0 & 0 & 0 & \rho g \iint x^2 dA + \rho g V_0 r_3^b & 0 \\ 0 & 0 & 0 & 0 & 0 & 0 \end{bmatrix} \quad (3.37)$$

Where:

- $V_0$  is the submerged volume
- $A_0$  is the cut-water plane area of the platform in un-displaced position



- $r_3^b$  is the vertical component of the position vector of the center of buoyancy in the un-displaced position of the platform

The excitation forces are:

$$q(t, x, \dot{x}) = q_{WI} + q_{1WA} + q_{2WA} + q_{CU} + q_{ext} \quad (3.38)$$

To solve equation 3.27, there exists two methods: convolution integral and separation of forces.

### 3.6.1 Convolution Integral

Equation 3.27 is re-arranged into:

$$m + A(\omega)\ddot{x} + C(\omega)\dot{x} + Kx = f'(t) = q - D_2f(\dot{x}) - D_1\dot{x} \quad (3.39)$$

Where the frequency-dependent coefficients are used to write the dynamic equilibrium equation:

$$A(\omega)\ddot{x} + C(\omega)\dot{x} = f(t) = f'(t) - Kx - m\ddot{x} \quad (3.40)$$

For the frequency domain, the equation becomes:

$$(i\omega A(\omega) + C(\omega))i\omega X(\omega) = F(\omega) \quad (3.41)$$

Introducing  $A_\infty$  and  $C_\infty$ , the equation becomes:

$$-\omega^2 A_\infty X(\omega) + (i\omega a(\omega) + c(\omega))i\omega X(\omega) = F(\omega) \quad (3.42)$$

Then by introducing Fourier Transform the main equation of motion becomes:

$$(m + A_\infty)\ddot{x} + D_1\dot{x} + D_2f(\dot{x}) + Kx + \int_0^t h(t - \tau)\dot{x}(\tau)d\tau = q(t, x, \dot{x}) \quad (3.43)$$

The above form can be used to find the frequency-dependent mass and damping however these concepts have been discussed earlier so they will not be explored further.

### 3.6.2 Separation of Motions

This method separates the equation of motion into high frequency ( $q^{(1)}$ ) and low frequency ( $q^{(2)}$ ) parts. The high frequency part is solved in the frequency domain.

$$\begin{aligned} q(t, x, \dot{x}) &= q^{(1)} + q^{(2)} \\ q^{(1)} &= q_{1WA} \\ q^{(2)} &= q_{WI} + q_{2WA} + q_{CU} + q_{ext} \end{aligned} \quad (3.44)$$

The position vector separates to:

$$x = x_{Low\ Frequency(LF)} + x_{High\ Frequency(HF)} \quad (3.45)$$

The high frequency motion becomes:

$$X_{HF}(\omega) = \left( -\omega^2(m + A(\omega)) + i\omega D_1 + C(\omega) + K \right)^{-1} H_1(\omega) \zeta(w) \quad (3.46)$$

The low frequency motion becomes:

$$\begin{aligned} m + A(\omega = 0) \ddot{x}_{LF} + D_1 \dot{x}_{LF} + D_2 f(\dot{x}) + K x_{LF} &= q^{(2)} \\ &= q_{WI} + q_{2WA} + q_{CU} + q_{ext} \end{aligned} \quad (3.47)$$

### 3.7 Anchor lines (Catenary System)

The FOWT will be moored using three mooring lines that will be used in calculation of the location of the vessel.

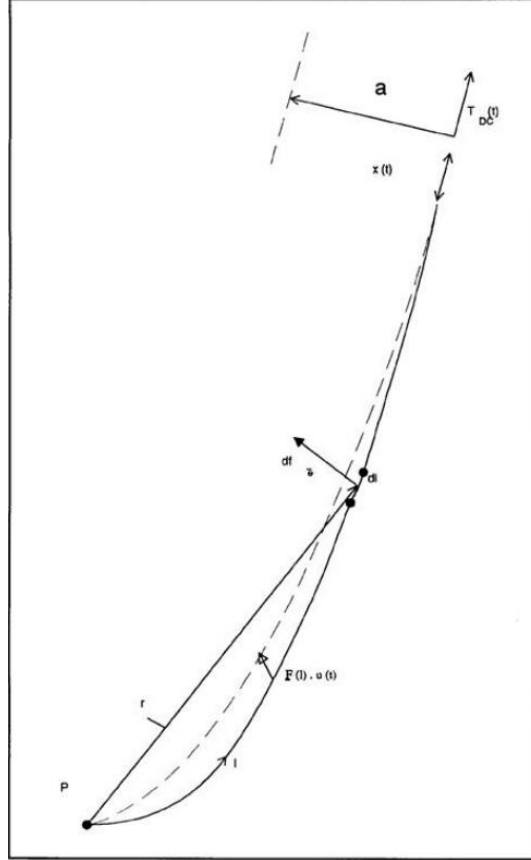


**Figure 3.3:** Dynamic Tension Computation Model

In the figure above, Point P is the point at which the mooring line contacts the seafloor. The mooring line has mass thus creating dampening, tension and thus motion. The moment equilibrium with respect to point P must be written and used to solve the mooring line equation:

$$\int_0^S |d\vec{f}_c \times \vec{r}| dl = a T_{DC} \quad (3.48)$$

$$T_{DC} = k^E(x - u) - k^G u \quad (3.49)$$

The line motion can be expressed by manipulating the motion equation:

$$c^* \dot{u} |\dot{u}| + k^* u = k^E x \quad (3.50)$$

Where:

- $c^*$  is the generalized line damping
- $k^*$  is the generalized line stiffness
- $k^E$  is the axial line stiffness
- $k^G$  is the geometric catenary stiffness
- $u$  is the displacement
- $\dot{u}$  is the velocity
- $x$  is the tangential motion excitation of the line end for the mooring line.

### 3.8 Equations of motion

These are the laws that govern the solution for the positioning of the vessel. The Linear Momentum, denoted by  $P_B$ , is due to external forces. The Angular Momentum, denoted by  $L_B$  is due to the external moment. The angular momentum and external moment are to be about the same reference point, globally (0,0,0).

$$\begin{aligned} P_B &= (m(v + w \times r_c)) \\ L_B &= I\omega + m r_c \times v \end{aligned} \quad (3.51)$$

Where:

- $m$  is mass
- $v$  is velocity
- $\omega$  is angular velocity
- $r_c$  is the position of the centre of mass with respect to the body origin
- $I$  is the body inertia tensor. Mass Moment of Inertia can be explained as the product of the mass of a part of a structure and its relative distance to the centre of gravity (ToolBox, 2022):

$$I = \sum_i m_i r_i^2 = m_1 r_1^2 + m_2 r_2^2 + m_3 r_3^2 + \dots + m_n r_n^2 \quad (3.52)$$

$$\begin{aligned} P'_B + \omega \times P_B &= F \\ L'_B + \omega \times L_B + v \times P_B &= M \end{aligned} \quad (3.53)$$

By using these equalities, we can introduce matrices which hold information about the 3D position and mass. Since the forces acting upon the vessel come in all directions and cause movement in all directions the above equations can be transformed into the following:

$$V = \begin{bmatrix} V_{11} & V_{12} \\ V_{21} & V_{22} \end{bmatrix} = \begin{bmatrix} A_{11} + B_{11} & A_{12} + B_{12} \\ A_{21} + B_{21} & A_{22} + B_{22} \end{bmatrix} = A + B \quad (3.54)$$

Where A is the added inertia matrix and B is the body mass matrix

$$\begin{bmatrix} P \\ L \end{bmatrix} = V \begin{bmatrix} v \\ \omega \end{bmatrix} \quad (3.55)$$

The accelerations become:

$$\begin{bmatrix} \dot{v} \\ \dot{\omega} \end{bmatrix} = V^{-1} \begin{bmatrix} \omega \times P + F_1 \\ -\omega \times L - v \times P + M_1 \end{bmatrix} + \begin{bmatrix} \omega v \\ 0 \end{bmatrix} \quad (3.56)$$

### 3.9 Positioning

Creating the environmental effects, calculating their effects (dampening etc...), using them in the equation of motion and finally solving the kinetics allow for understanding the positioning of the vessel at a given time. The position vector of the body can be written as:

$$x = (x, y, z, \phi, \theta, \psi) \quad (3.57)$$

By allowing for the creation of a relationship between the environment and the vessel, a complex system can be created to understand the changing position. Then the modified Euler method, 3<sup>rd</sup>-order Runge-Kutta-like method or the Newmark-Beta predictor-corrector method can be used to solve the complex equation.

## 4 Simulation Procedure

From the literature survey, the requirements are defined, so are the constraints. At this point the process starts with using GeniE software to define the FEM models and prep them for the other modules.

### 4.1 Sesam Manager

The Sesam Manager is the interface between all other modules. This ensures a quick, easy, and seamless transition between modules as well as creating/organizing a workflow. The modules which are listed allow for the user to view the selection of modules. In Chapter 2, the usage of the best fitting module was discussed in depth. The modules that are required are now placed to have one output from one module to integrate with the other.

The selected modules are placed one after the other to create a workflow between modules. This process is explained in detail in both the Sesam Feature Description booklet as well as in the Sesam Manager explanatory video (DNV, 2022). The workflow which is designed follows the same procedure in this thesis, GeniE which is followed by Hydro-D which is followed by Sima.

### 4.2 GeniE

Genie software allows for FEM file input. The T1 (Morison model), T2 (panel model), T5 (mass model) are imported into the software. While the importing happens, the GeniE import screen allows for repairing of breaking elements. This is an important aspect as the message viewer outputs the final importing result with possible breaks in the actual model, thus by running this repair option with 0 warnings, it is evident that the model does not have major flaws. After all models are imported, they can be viewed in the 3D editor.

After all models have been imported, they are subjected to an analysis. This analysis will create the mesh and make sure the output FEM file can be used as inputs in Hydro-D for the hydrodynamical coefficients needed.

FEM (Finite Element Method) models are models in which the mathematical equations are set up so that the differential mathematical problems can be solved numerically (Mansur, et al., 2004). One of the equations that can be exemplified is the Navier-Stokes momentum equation (Constantin & Ciprian, 1989):

$$\begin{aligned} \rho \left( \frac{\partial u}{\partial t} + u \cdot \nabla u \right) \\ = -\nabla p + \nabla \cdot \left\{ \mu \left[ \nabla u + (\nabla u)^T - \frac{2}{3} (\nabla \cdot u) I \right] + \zeta (\nabla \cdot u) I \right\} + \rho g \end{aligned} \quad (4.1)$$

For the purposes of this thesis, an in-depth look at how GeniE will set up the FEM models will not be discussed.

The GeniE output can be found in the workplace folder as a FEM file. All three models are taken from the workspace folder individually for use in Hydro-D.

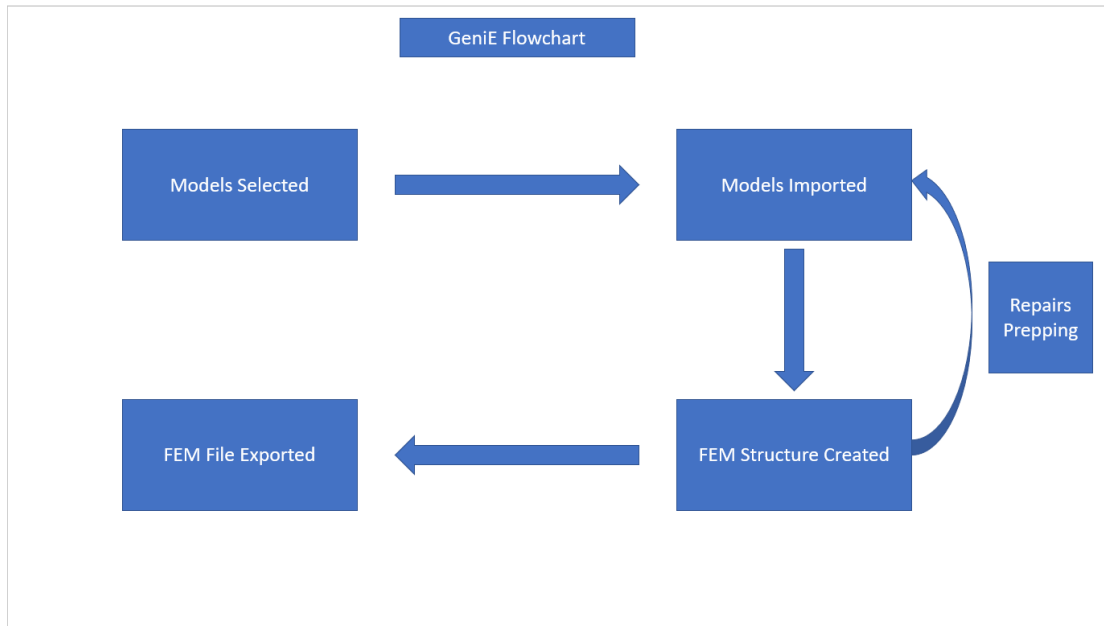


**Figure 4.1:** GeniE Flowchart

## 4.3 Hydro-D

Hydro-D is the main module where the previously discussed hydrodynamic coefficients are taken from. Hydro-D has two main analysis tools: Stability and Wadam analysis. There are four other analyses: Stability Rule Check, Max Kg Analysis, Strength Analysis, Limit Surface. Even though these analyses provide great insight into the behaviors of the FOWT, they will not be considered for the scope of this thesis. The analysis that will be focused on will be Wadam analysis. To construct a Wadam analysis takes many steps.

### 4.3.1 Wadam Analysis Creation

Wadam will be the main output from Hydro-D to Sima. To get the required WAMIT.out file and the GDF Geometry output file, many steps need to be taken first.

#### 4.3.1.1 Wadam Analysis Parameters

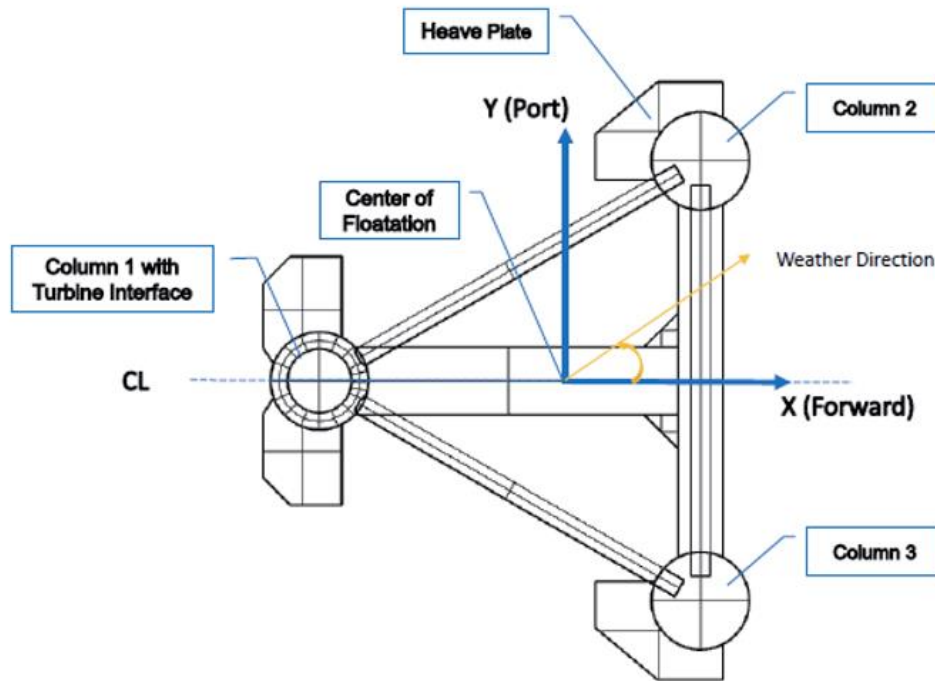
The condition is set to Frequency domain condition as the given input data and the required output data is required in this condition type. Load transfer is also included to get the required pressure and loads on the panels. Panel model is included to ensure the Panel Model is included in the analysis for the GDF geometry. Morison model is also included to get the Morison-like loading effect.

#### 4.3.1.2 Creating Direction Set

A Directions folder must be created for the Direction Set to be created. In the Directions folder, the Direction Set is created. The directions created have been discussed previously in chapter 1.4. The reasoning behind this is both based on computational cost and proposed direction sets by Hydro-D as well. The direction scope is from 0 to 360 as the FOWT is stationary and is receiving waves, wind and current from all around. Some applications are limited to moving ships that are only assessed in the 0-to-180-degree scope while the ship is moving towards the 90-degree angle, some are

from -90 (270) to 90 degrees where the ship is moving in the 0-degree x direction. The reasoning behind all these differences is based on literature as well as previous assessments which have different results. It is important to note the direction with which our FOWT will be facing.

II



¶

**Figure 4.2:** FOWT Facing Direction

As can be observed in figure 4.2, the front of the FOWT is to face the 0-degree angle.

### 4.3.1.3 Creating Frequency Set

A frequency set must be created for the Frequency Domain to be created. The frequency set is created according to the period set. The frequency set is vital for the creation and calculation of the zero and infinite frequency added mass results. The infinite frequency added mass equations is dependent on the  $f$  variable. The  $f$  variable being the frequency itself. Thus, this frequency set is the fundamental variable on which the matrices for the zero and infinite frequency added mass will be built. However, in the format presented in Hydro-D, the frequency set can be directly input as either wave period, wavelength, or frequency. To test the frequencies from differing range one can input any frequencies to obtain different results. In the Hydro-D user manual, there is a set of proposed Period tables (DNVGL, 2022). Since a range or alternatively a set of frequencies are not given by the problem definition, nor can it be directly guessed/calculated (since the severe weather patterns are to be analyzed and the general weather conditions are made in non-linear and generated format with many various frequencies and wavelengths) it is better to use the proposed Period settings.

**Table 4.1:** Wave Period Settings

From	To	Step
5 seconds	30 Seconds	5 seconds

#### 4.3.1.4 Location Setting

The location properties must be input as these values are the base values for the whole simulation. One of the most important inputs is the water depth as these effects the shallow or deep-water effects. Location values also include water and air values. The water and air density values are also crucial as these values have a direct impact on the simulation. An important note is that the gravity setting must be very accurate as the WAMIT.out file contains this value and carries it over to Sima, (DNV, 2022), thus the value presented in the gravity, density and kinematic viscosity setting must match those that are viewed in Sima.

**Table 4.2:** Location Variables and Values

Location Variables	Value
<b>Gravity</b>	9.8066 m/s <sup>2</sup>
<b>Water Depth</b>	100 m
<b>Water Density</b>	1025 kg/m <sup>3</sup>
<b>Water Kinematic Viscosity</b>	1.19E-06 m <sup>2</sup> /s
<b>Air Density</b>	1.222 kg/m <sup>3</sup>
<b>Air Kinematic Viscosity</b>	1.462E-05 m <sup>2</sup> /s

#### 4.3.1.5 Frequency Domain Condition

The Frequency Domain Condition is dependent on the direction set and the frequency set. Simply put, the Frequency Domain is an analysis type that is a method of solving mathematical problems and equations with respect to frequency rather than time. This simplifies many problems as incorporating the sinusoidal wave function with a given frequency into a simulation where the kinematics of waves are at hand is much easier than solving the problem with relation to time. The principle behind this is by using a Fourier Transform, one can break down a function into smaller sinusoidal “waves”. By implementing this procedure, complex functions such as wave functions can be expressed as the assembly of smaller simpler functions. The Fourier Transform of a function  $g(t)$  can be expressed as:

$$F\{g(t)\} = G(f) = \int_{-\infty}^{\infty} g(t)e^{-2ift} dt \quad (4.2)$$

As is evident, the purpose is to transform the function  $g(t)$  which is dependent on time to the function  $G(f)$  which is dependent on frequency. Let us examine a function of  $g(t)$  which is a wave that has an amplitude of  $A$  for  $[-T/2, T/2]$  and is 0 elsewhere.

$$\begin{aligned}
F\{g(t)\} = G(f) &= \int_{-\infty}^{\infty} g(t)e^{-2\pi ift} dt = \int_{-\frac{T}{2}}^{\frac{T}{2}} Ae^{-2\pi ift} dt \\
&= \frac{A}{-2\pi if} \left[ e^{-2\pi ift} \right]_{-\frac{T}{2}}^{\frac{T}{2}} = \frac{A}{-2\pi if} [e^{-\pi ifT} - e^{\pi ifT}] \\
&= \frac{AT}{\pi fT} \left[ \frac{e^{-\pi ifT} - e^{\pi ifT}}{2i} \right] = \frac{AT}{\pi fT} \sin(\pi fT) = AT[\text{sinc}(fT)]
\end{aligned} \quad (4.3)$$

Thus, by using the Fourier Transform, we can deduce hard equations to smaller easier “chunks” that require less computational power (Byju's, 2022). In Hydro-D, there are



two options, the first is adding a deterministic condition which requires more data that must be assumed/taken from literature, which will create a higher margin of error, or secondly add a frequency domain condition which is only set by using the direction set and frequency set. The frequency domain condition will be used to apply the WADAM analysis.

#### 4.3.1.6 Hydro Model Creation

The hydro model is now edited to be able to be called in and edited. The baseline z-coordinate must be declared to define the parameters where the Hydro Model will be evaluated. A general Aft Perpendicular x coordinate will be given to provide the necessary parameter. A Forward Perpendicular will also be declared to provide the limits of the investigation. From this the LPP is calculated as  $LPP = |FP-AP|$ . There is the choice to specify the MODU (Mobile Offshore Drilling Unit) type. The MODU type is for drilling structures. As the model is a FOWT, the model is not considered to be a MODU (USCG, 2022).

**Table 4.3:** Coordinate System Specifications

Coordinate System	Values
<b>Baseline z-coordinate</b>	0 m
<b>AP(x)</b>	0 m
<b>FP(x)</b>	100 m
<b>LPP (Calculated)</b>	100 m

#### 4.3.1.7 Element Model Creation

At this step, the three models that have been meshed in GeniE are now input as element models. T1, T2 and T5 are seamlessly imported into Hydro-D. These element models will later be called in Panel model definition for the hydro model. The Morison model is then exported into the hydro model.

The system model is composed of smaller pieces of Element models. These element models provide an interaction between the nodal variables and loads in the element. These loads are used to calculate the nodal variables (Zhuming Bi, 2019). These element models are then used together to create the System Model.

The Morison Model is used to apply the drag forces by computing the force per length of body (Morison, et al., 1950). The Morison drag force calculation has been discussed earlier.

#### 4.3.1.8 Loading Condition Creation

The Loading Condition is crucial to set up as the waterline is set with possible trim. The Loading Condition represents the initial state of the FOWT. Since the models given are the pieces of the vessel below the WT (Water Line), the Waterline Z is set to the height of the models, 18 meters. There are two methods of specifying the Loading Condition: by inputting the Waterline & Trim, or by inputting the Drafts. The first option is implemented by setting the Waterline Z to 18 meters and then inputting 0-degree trim to ensure that the case represented is used to get the hydrodynamic coefficients. The second method is used more commonly by ships or in a situation

where computing the trim is required/necessary and the trim is not provided. The Loading Condition is set in the environment specified by the Location Setting.

**Table 4.4:** Loading Condition Specifications

Loading Condition Variables	Values/Preferences
<b>Specification Type</b>	Waterline & Trim
<b>Waterline Z</b>	18 m
<b>Trim angle</b>	0 degrees

#### 4.3.1.9 Mass Model

The mass model is imported as an element model alike to the Panel and Morison model. The Mass Model has been discussed earlier. It is important to note that the mass model consists of minor nodes that have mass data which are used to calculate the forces that are subjected onto the FOWT.

### 4.3.2 Wadam Analysis Execution

The execution of the Wadam analysis is important to set up properly as the default settings are insufficient to the required outputs from the thesis' problem definition.

#### 4.3.2.1 Wadam Analysis General

The general tab of the Wadam analysis specifies the hydro model, loading conditions, environment condition and the sea state (optional). The sea state is not included in this analysis as it is not required, and not enough input data is provided. The boundary type is specified according to the type of structure, which is floating. The constraints are default settings and are adequate. The motion reference point is set to global origin as the model is set accordingly. It is possible for the motion reference point to be moved but it is important to re-locate the vessel in any other module that will be used.

#### 4.3.2.2 Wadam Analysis Output

The Output ribbon specifies the output file types. The Load transfer file is binary or ASCII. Unformatted option (binary is chosen). The Global response file is set to SIF (Standard Interchange Format) as this is used in Sima as an input. The print level is set to Load Distribution so that the required values are taken without the need of excess data. Hydro-D can provide Maximum print; however, it is important to note that the data output may be more than expected. The crucial box that must be ticked is the "Save temp. Wamit files" option as it allows for WAMIT.out file to be created which has most of the input files for Sima. The temp. wamit files are also a great indicator of whether something has gone wrong in the simulation. The wamit file has an array of data. One of which is very crucial: the volume in the x, y, and z direction. These three values must coincide or there is a trim in the model which could be a problem in the buoyancy and weight definition.

#### 4.3.2.3 Wadam Analysis Load

This ribbon enables to add the "Load transfer" box. This will allow the user to view the results in Xtract. Xtract is an inbuilt post-processor. The load transfer to the structural model is an important choice. There are three choices: Shell/solid, Beam and

Composite. Shell/solid choice makes the panel loads are transferred to the shell/solid elements (Panel Model) of the structure. Beam structural model choice makes the beam loads transferred to the specified structural model. It is required that the Morison model is a subset of the structural model (or simply be the same model), i.e., the beam elements in the Morison model must be identical to the corresponding elements in the structural model. Also, both element and node numbers must be identical. The structure mode may however include additional elements. If the composite model is selected, the Morison model is used as the beam model. Morison loads are transferred to the Morison model. This means that the Morison model must either be a super element in the Structure model or be the same model. Panel loads are transferred to the shell/solid elements of the structural model. This choice is explained in further detail in the Hydro-D user manual (DNVGL, 2019).

### 4.3.3 Wadam Analysis Results

The results for the analysis can be viewed in Xtract or by the text files.

#### 4.3.3.1 Wadam Analysis Results viewed in Xtract

The results in Xtract can be viewed by the displacement and the load distribution on the panels. Figure 9.5 presents the FOWT under the effects of weather direction 0 degrees. The scale is from blue (low stress) to red (high stress). The results in Xtract (Figure 9.6) can be viewed for either every phase or for every weather degree. The results are too massive to be shown here, also the results from this analysis are to be used specifically in Sima, thus are only viewed to make sure the model is being subjected to loads and is causing deflection and movement.

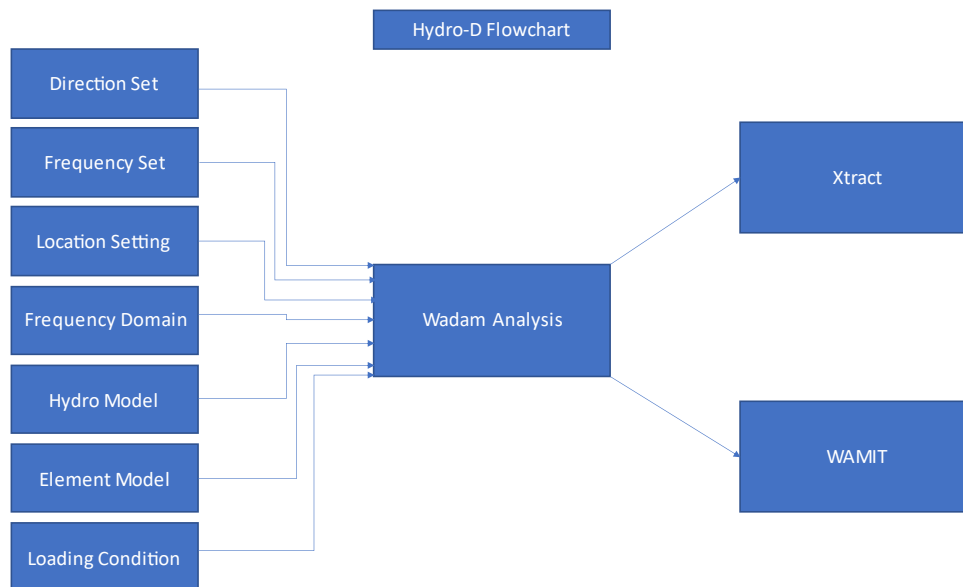


**Figure 4.3:** Hydro-D Flowchart

## 4.4 Sima

Sima is the final tool that will be used in the workflow. The Sima software can create dynamic analysis. The effects of weather are defined in detail in Sima as the total effects are coupled in a time-domain simulation.

#### 4.4.1 Simulation Choice

Sima provides many sub-modules: Fatigue analysis task, Metocean task, Post Processor task, Riflex task, Report task, Simo task, Storage task, Verification task, Wamit task, Windfield task and workflow task. The Simo task is the task which will simulate the dynamic response of the substructure tied with the catenary system and the RNA.

#### 4.4.2 Simo Task Location

Sea Surface configuration is by 1 kilometer to 1 kilometer size by default. This is more than enough to make the required simulations. A larger area may be defined for unmoored vessels or for larger floaters with looser mooring lines etc. The Flat Bottom configuration matches the Sea Surface configuration by default in size except for the Z setting. This option shows the depth of the flat bottom. This is the same as the depth option in Hydro-D and is set to -100 meters.

#### 4.4.3 Simo Body Creation

After the location has been set, a body is created in the Simo task to show the actual floater body. This body has no kinetics so an error will show “body has no mass”.

##### 4.4.3.1 Importing Hydro-D Results

By using the created Wamit files from Hydro-D, the results are imported into the task. It is important to select “Import into existing task” option to seamlessly import the data. After Kinematics have been imported into the Simo task, the GDF geometry which was created in Hydro-D is imported.

##### 4.4.3.2 Checking Import

All data that is imported in Simo task is cross-checked before continuing the rest of the analysis.

#### 4.4.4 Catenary System

The Catenary system is the main mooring line system that keeps the substructure from floating off. The mooring system placement is specified by the given mooring line attachment and anchor placement data.

**Table 4.5:** Catenary System Input Table

Line No.	Azimuth	Fairlead [m]			Anchor [m]			Pretension [kN]	
	[°]	X	Y	Z	X	Y	Z	Total	Vertical
1	185	-40.25	-0.57	15.0	-402.37	-32.25	-100.0	354.34	306.44
2	175	-40.25	0.57	15.0	-402.37	32.25	-100.0	354.34	306.44
3	65	19.63	35.14	15.0	173.26	364.58	-100.0	354.34	306.44
4	55	20.62	34.57	15.0	229.11	332.34	-100.0	354.34	306.44
5	305	20.62	-34.57	15.0	229.11	-332.34	-100.0	354.34	306.44
6	295	19.63	-35.14	15.0	173.26	-364.58	-100.0	354.34	306.44

Sima allows for the catenary system to be created by either specifying an anchor location or by the pretension. For the purposes of this task, the anchor location will be used.

#### 4.4.4.1 Catenary System Mooring Line Specifications

The mooring lines themselves are made of four segments. The Top Chain, Mid Chain, Heavy Segment and Anchor Chain.

**Table 4.6:** Mooring Line Segments

Segment	Type	Diameter	Mass	EA	Length	MBL
		[mm]	[kg/m]	[MN]	[m]	[kN]
Top Chain	Studless	130	338	1420	32.5	13573
Mid Chain	Studless	130	338	1420	125	13573
Heavy Segment	Studless with clump weight	130	2055	1420	50	13573
Anchor Chain	Studless	130	338	1420	208	13573

These specifications are input into the “Segmented Line Types” part of the Catenary System.

**Table 4.7:** Segmented Line Type Specifications

Number of Horizontal Points (nph)					40		
Number of Vertical Points (nptv)					5		
Minimum Relative Z-Position (Vmin)					-1		
Maximum Relative Z-Position (Vmax)					1		
Minimum Horizontal Tension					0		
Maximum Tension					1.3573e+07		
Segments							
No	Num Elements	Length	Diameter	E mod	Em Fac	Uwia	Watfac
1	20	208	0.13	2.0e+11	2.0	3315.8	0.869
2	20	50	0.13	2.0e+11	2.0	20160	0.869
3	20	125	0.13	2.0e+11	2.0	3315.8	0.869
4	20	32.5	0.13	2.0e+11	2.0	3315.8	0.869

Where:

- **Number of Horizontal Points:** Number of points in the line characteristics matrix, offset variation in the horizontal plane.
- **Number of Vertical Points:** Number of points in the line characteristics matrix, offset variation in the vertical plane.
- **Minimum Relative Z-Position:** Min. relative z-pos. For which the line characteristics will be calculated.

- **Maximum Relative Z-Position:** Max. relative z-pos. For which the line characteristics will be calculated.
- **Minimum Horizontal Tension:** Minimum horizontal tension to be used for calculation of line characteristics. Note: the minimum tension is set to 0 so that the lower tension limit is calculated.
- **Maximum Tension:** Max tension to be used in line characteristics calculations. Note: this is set to the breaking limit of the line types.

#### 4.4.4.2 Catenary System Body Points

For the catenary system to be defined, the attachment of the mooring lines must be defined on the floater body. The values presented below are all in meter units.

**Table 4.8:** Attachment Point Specifications

Name	X Position	Y Position	Z Position
Att1	-40,25	-0,57	15
Att2	-40,25	0,57	15
Att3	19,63	35,14	15
Att4	20,62	34,57	15
Att5	20,62	-34,57	15
Att6	19,63	-35,14	15

#### 4.4.4.3 Catenary System Anchor Points

After the body points are created, the anchor-seabed attachment points must be added for the lines to be created. The anchor points are set to the values specified in Table 10.

#### 4.4.5 Slender Elements

The slender elements tab allows for the creation of objects which are coupled to the body. There are two ways of completing this step. In Riflex simulations, the user is allowed to input a complex slender system. In Simo this is simplified. The differences can be viewed in Figure 9.7.

**Table 4.9:** Tower Cross Section Specifications

No	Cross Section	Length	Acc length
1	tower23	2,9	2,9
2	tower22	2,8	5,7
3	tower21	2,7	8,4
4	tower20	2,7	11,1
5	tower19	2,7	13,8
6	tower18	2,7	16,5
7	tower17	2,7	19,2

8	tower16	2,7	21,9
9	tower15	2,7	24,6
10	tower14	2,7	27,3
11	tower13	2,7	30
12	tower12	2,8	32,8
13	tower11	2,8	35,6
14	tower10	2,7	38,3
15	tower9	2,7	41
16	tower8	2,7	43,7
17	tower7	2,7	46,4
18	tower6	2,7	49,1
19	tower5	2,7	51,8
20	tower4	2,7	54,5
21	tower3	2,7	57,2
22	tower2	2,7	59,9
23	tower1	2,8	62,7

**Table 4.10:** Simo Tower Configuration

Specific Volume	33,2
Distributed Mass	6771,4
Number of Strips	100
Mass	7,11E+05
Length	105
Volume	3486
COG X	-33,775
COG Y	0
COG Z	67,5

#### 4.4.6 The RNA

The nacelle assembly is introduced in Sima. Since GeniE was only used for meshing while Hydro-D is used for hydrodynamical properties, the Sima software will have to incorporate the effects of wind on the turbine blades and the nacelle. The case that will be tested is the storm case i.e., the turbine has stopped turning. This is an advantage as modelling the RNA would take substantial time if the input for the turbine is not given. To solve the absence of the RNA, a simple disc model is considered. The simple disc model is to create an area with the quadratic wind coefficients which will be required to model the effects of wind on the FOWT. The disc model is then moved to a cylinder model to get the 360-degree effects of wind on the FOWT.

The cylindrical setup shown in Figure 9.8 is however re-considered since the true effects of wind are not captured with high enough accuracy. To make the actual blade geometry and implement it within the Simo application would take substantial time, thus another alternative must be chosen.

#### 4.4.6.1 Dummy Tower

The Simo application provides an example RNA setup. The specifications have the inputs for an actual tower with given tower controller specifications. The environmental status is that of a storm. Thus, the controller of the wind turbine has been deleted and replaced with a very high rotational stiffness. In the problem definition the tower has a cut off speed of 25 m/s provided by the manufacturer. This is the reason it is known that the hub will not be rotating. The hub itself is attached to the floater body via docking cones which will ensure the stability of the hub while high wind conditions are present. A quadratic wind coefficients matrix will also be assigned to ensure that the whole sweeping wind area is taken into consideration by the simulation. The attached blades have been altered to meet the exact length and mass of that in the actual tower. The RNA can be viewed in Figure 9.9.

#### 4.4.6.2 Hub Attachment

The hub is attached via docking cones, a thrust specification and a moment coupling between the hub and the floater body. This is done to ensure that the moment created by the wind is transferred to the actual floater body to get the correct dynamical response.

### 4.4.7 Environment Specifications

The environment values are input according to the specifications provided by the problem definition.

**Table 4.11:** Wind Wave Configuration

Wind Wave				
Direction	Spreading type	Number of Directions	Significant Wave Height	Peak Period
0	Unidirectional	1	14,72	11,67

**Table 4.12:** Swell Wave Configuration

Swell Wave					
Direction	Spreading type	Number of Directions	Significant Wave Height	Peak Period	Gamma
0	Unidirectional	1	14,72	11,67	2,23

**Table 4.13:** Wind Configuration

Wind		
Horizontal Velocity	Vertical Velocity	Direction
44,248	0,003322	0

**Table 4.14:** Current Configuration

Current			
No	Level	Direction	Velocity
1	0	0	1,34



2	-20	0	1,18
3	-28	0	1,09
4	-36	0	1,04
5	-45	0	0,99
6	-53	0	0,97
7	-61	0	0,95
8	-70	0	0,9
9	-78	0	0,86
10	-86	0	0,83
11	-97	0	0,71
12	-100	0	0

#### 4.4.8 The Simulation

Finally, after all the inputs, the static and dynamic simulations are run via inserting the initial and dynamic inputs that have been discussed earlier. Simo can visualize the simulation via the set-up menu in the dynamic simulation tab.

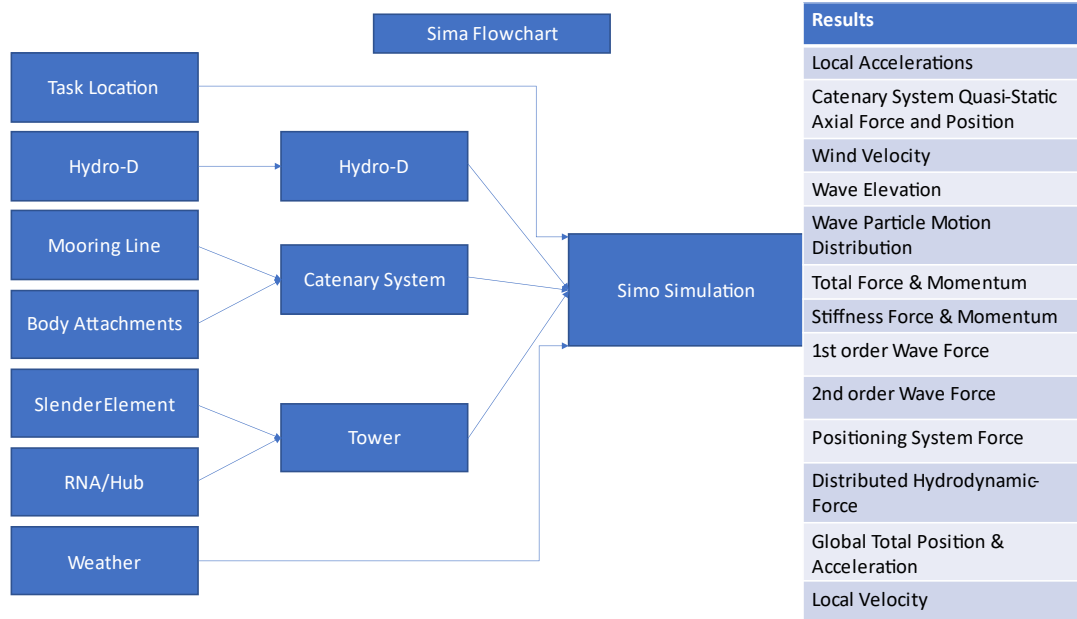


**Figure 4.4:** Sima Flowchart

## 5 Results

The results from Simo dynamic simulation will be presented. The main results which will be considered will be the positioning of the vessel in 3600 seconds. The change in  $x$ ,  $y$ ,  $z$ , roll, pitch, and yaw will be reported as well as their standard deviations.

The results which are presented in this chapter are relevant to the actual required dynamic response. Since the objective is to validate the SESAM simulation of the vessel by cross-referencing with Orcaflex, there must be a way of comparing results. The figures below show the change of the vessel in the  $X$ ,  $Y$  and  $Z$  direction as well as the Roll, Yaw, and Pitch. The visualization of the movement directions or also referred as degrees of freedom, can be viewed as below:

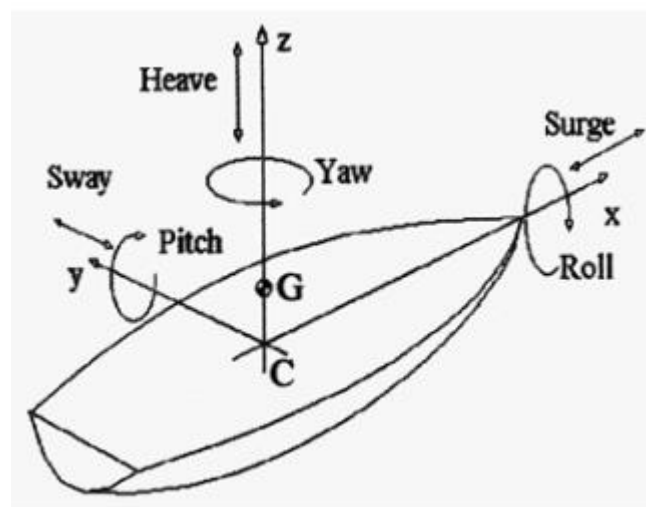


**Figure 5.1:** Movement Directions (Hermenau, 2013)

The weather impact is caused by three main components: wind, current and wave. Since the wind and current have a static relationship i.e., the wind is constant and current is a profile which doesn't fluctuate, the reason for fluctuations in the movement is due to the generated waves and thus the wave elevation. The theory behind the effect of the waves is explained in Chapter 3. After all the environmental effects are subjected to the vessel i.e., Chapter 4, this Chapter shows direct results of the theory. For reference, the wind, current and wave profile/elevation can be viewed:

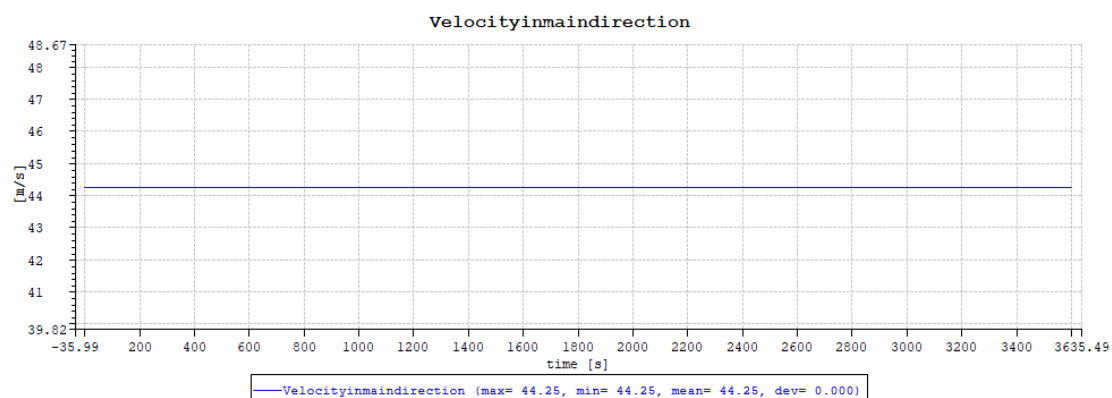


**Figure 5.2:** Wind Profile

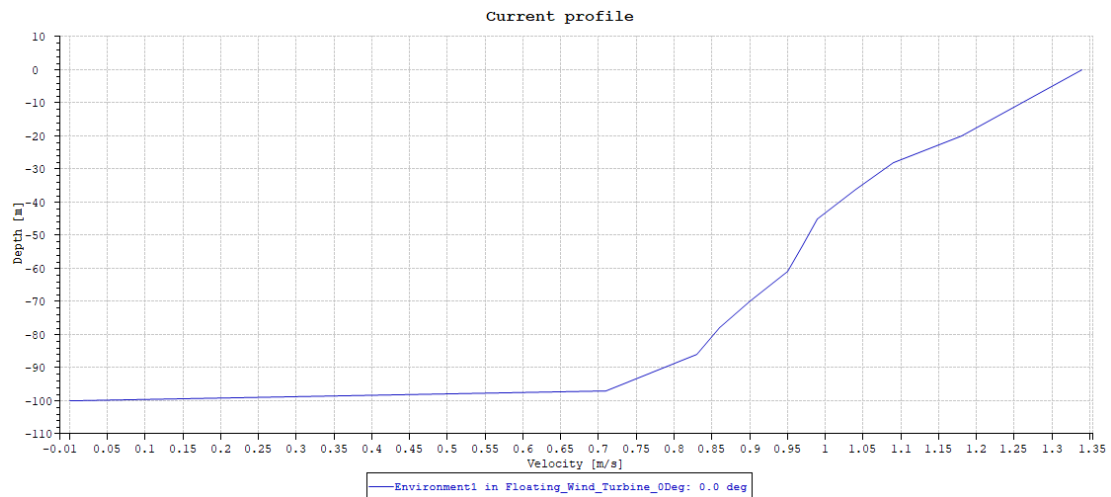


**Figure 5.3:** Current Profile

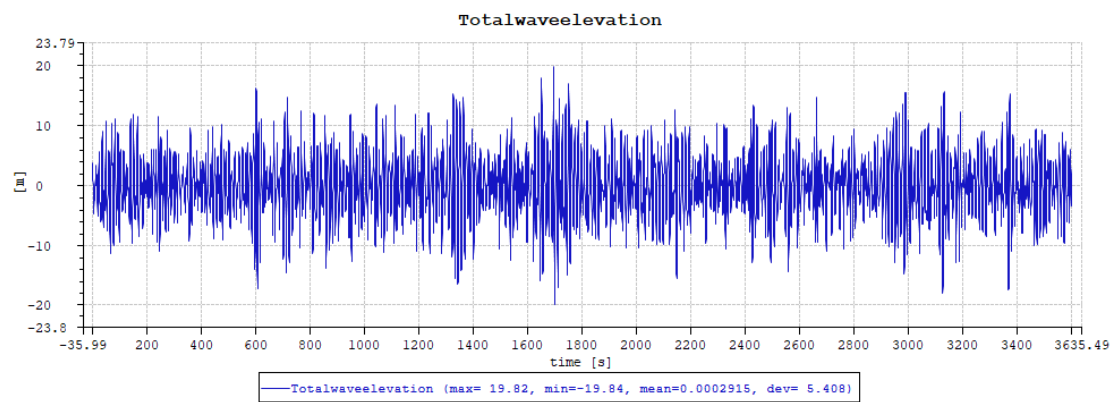


**Figure 5.4:** Wave Elevation

The effect of waves is the major driving force. The waves try to displace the vessel in the weather direction, the only force that allows for the vessel to stay in place is the mooring lines. The vessel is also subjected to dampening and hydro-static stiffness thus creating a time difference in reactions. For instance, looking at the wave elevation at the time interval ~20 to ~60 second where the initial effects are viewed, the difference of effects can be seen.

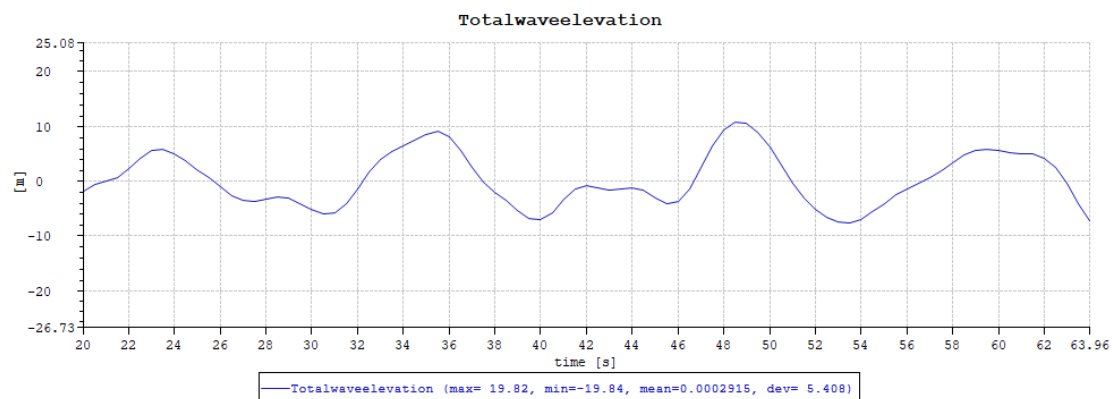


**Figure 5.5:** Wave Elevation between 20 and 60 seconds

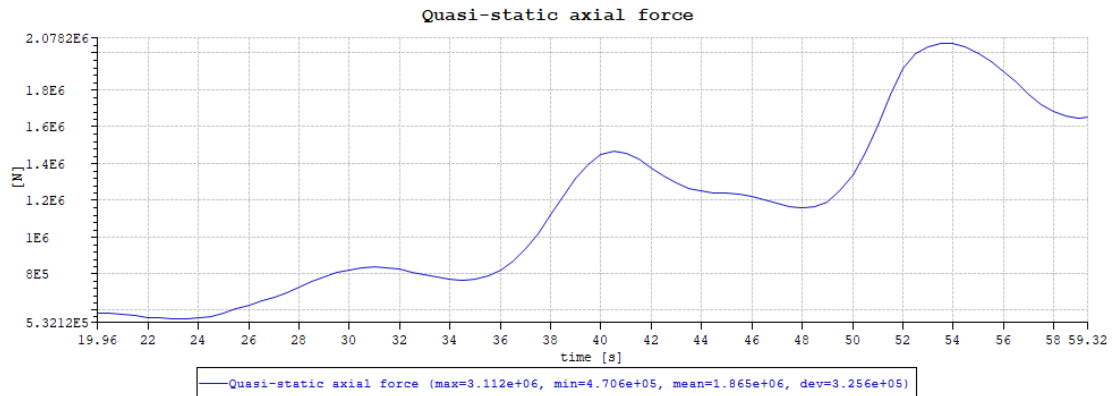


**Figure 5.6:** Quasi-static Axial Force at Element 4

The above graph happens at Element 4 of Catenary Line 1, which is the point at which is closest to the vessel. The Force rises from 5.32E5 to 2.07E6 Newtons in about 40 seconds.

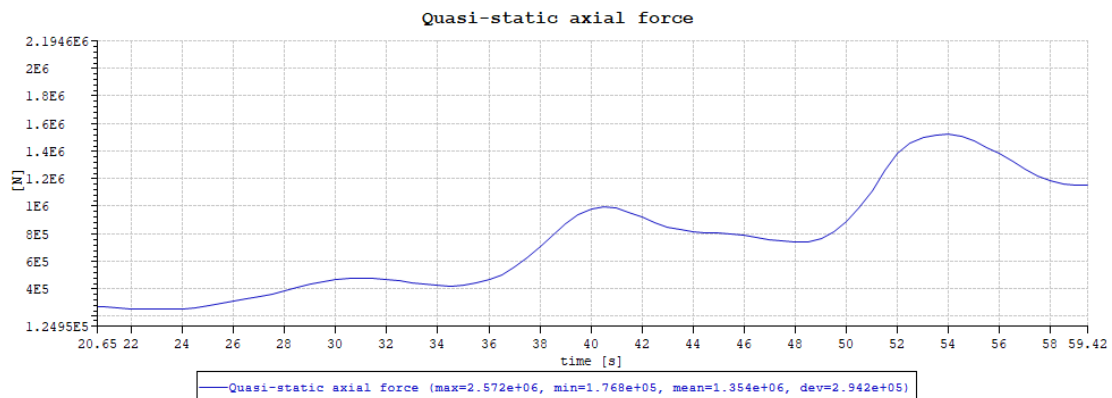


**Figure 5.7:** Quasi-static Axial Force at Element 1

The above graph happens at Element 1 of Catenary Line 1, which is the point at which is furthest to the vessel. The Force rises from 2E5 to 1.5E6 Newtons in about 40 seconds.

Thus, these wave effects and mooring line tension values create an ebb and flow which allow for the graphs to have changing values due to changing wave elevations and mooring line tension values. The total force in the X direction (for the 0-degree weather direction) can be viewed below.

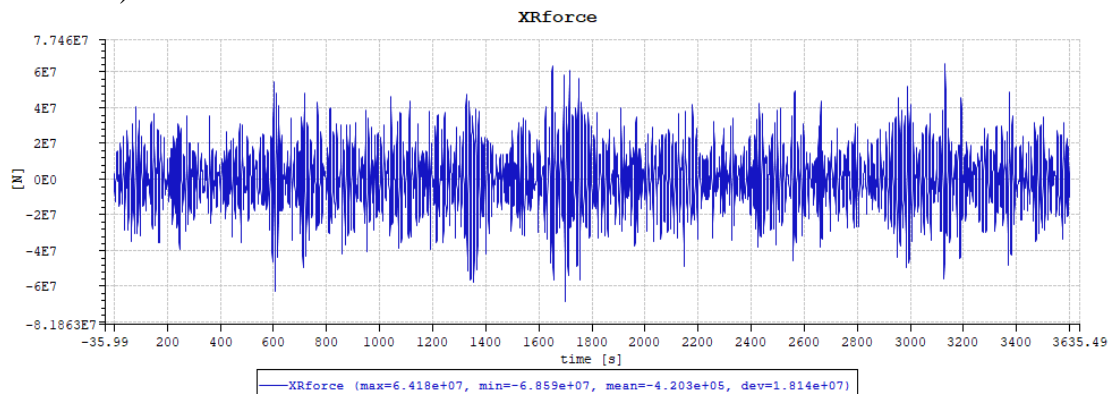


**Figure 5.8:** Total Force in the X Direction

From Newton's laws of physics, due to the changes and imbalances in forces the vessel oscillates in movement.

## 5.1 0 Degree Direction

The 0-degree weather direction is the initial start of the simulation. The weather direction is the degree difference from the X axis, recall Figure 4.2.

**X:**

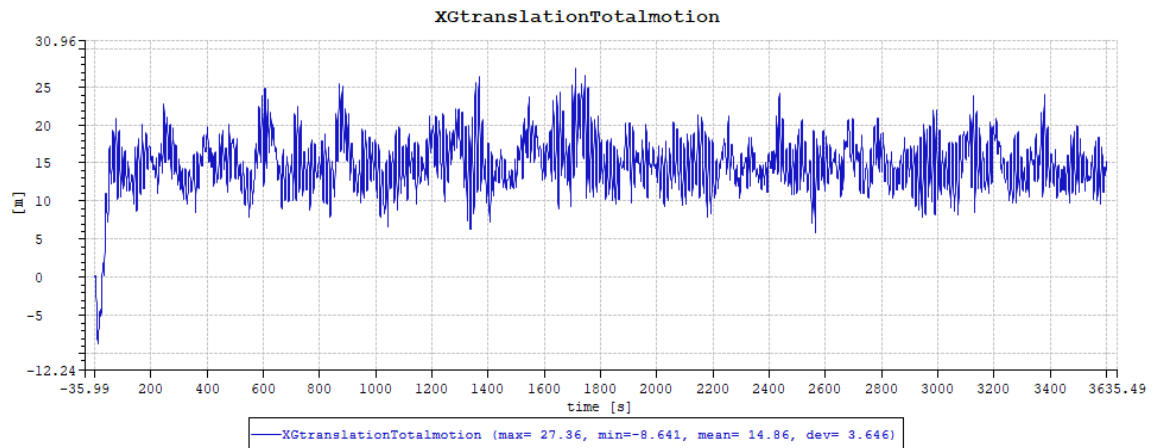


Figure 5.9: Change in X direction 0 Degrees

**Y:**

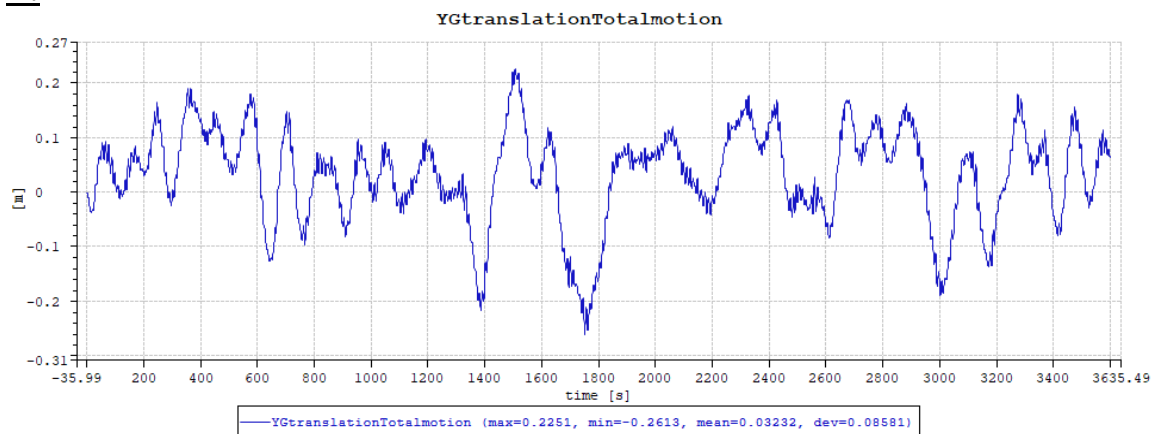


Figure 5.10: Change in Y direction 0 Degrees

**Z:**

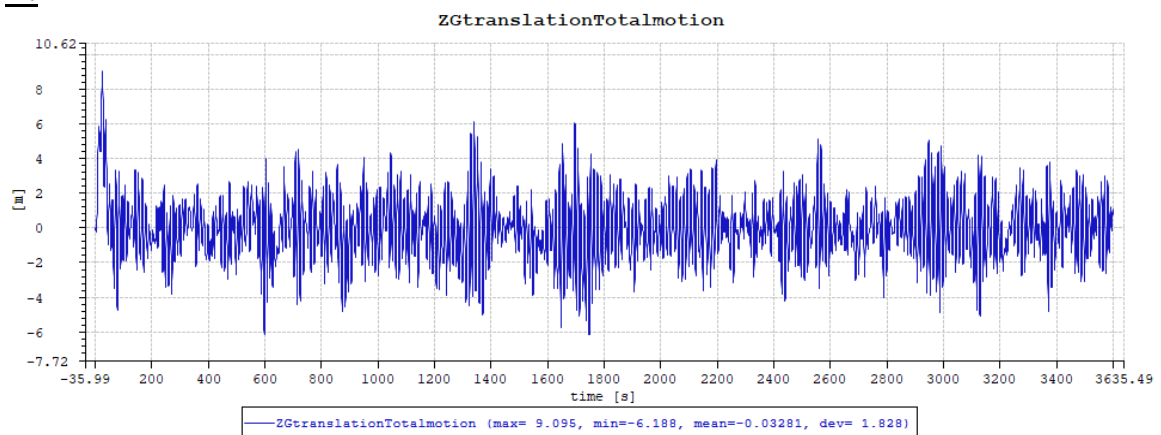


Figure 5.11: Change in Z direction 0 Degrees

### Roll:

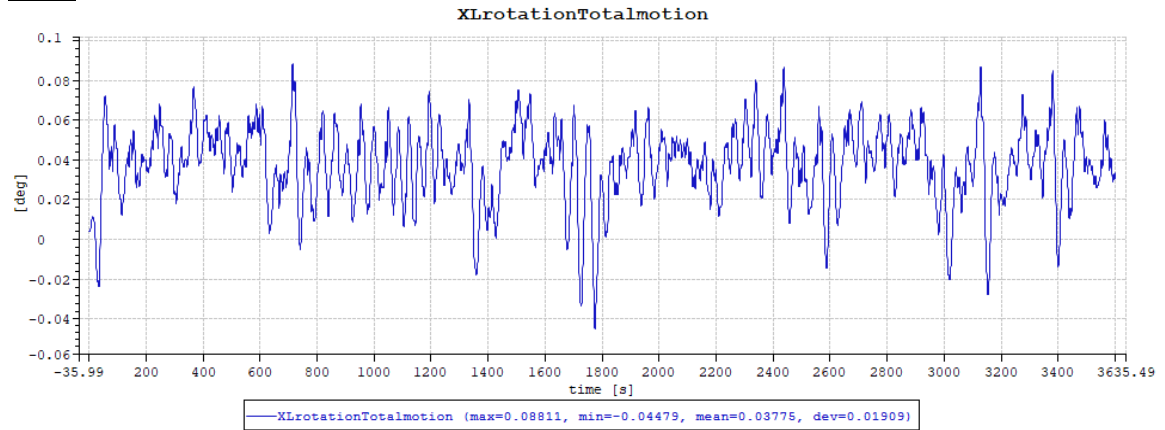


Figure 5.12: Change in Roll 0 Degrees

### Pitch:

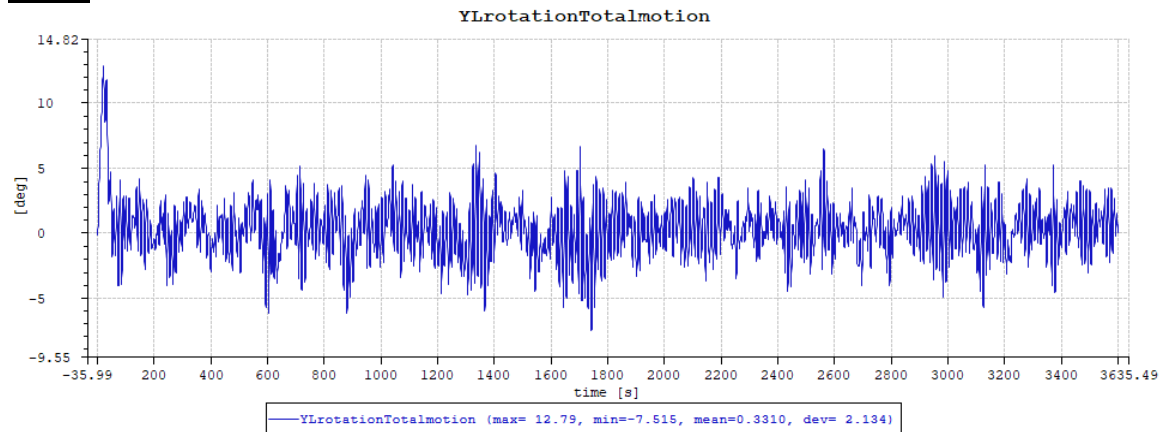


Figure 5.13: Change in Pitch 0 Degrees

### Yaw:

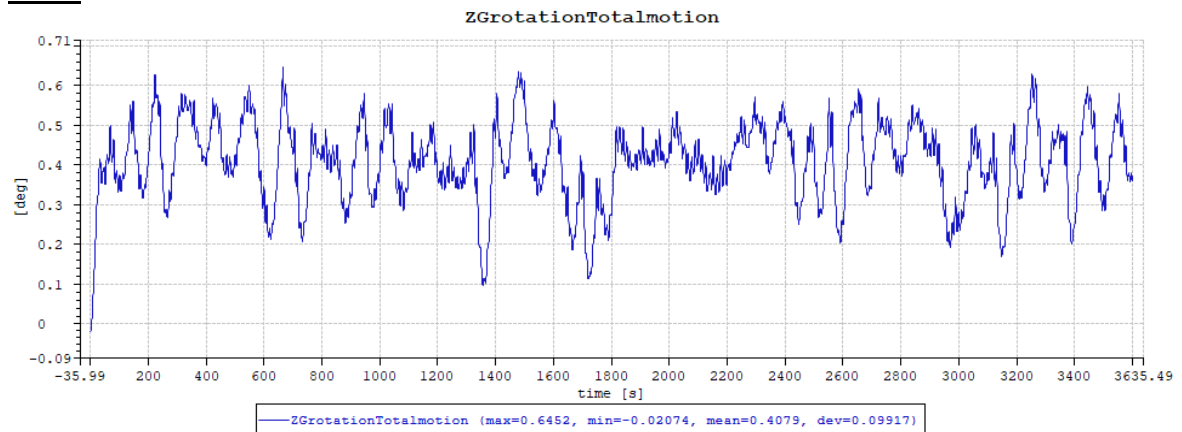


Figure 5.14: Change in Yaw 0 Degrees

## 5.2 30 Degree Direction

The 30-degree direction is where the change in the Y direction as well as Yaw starts to become more and more recognizable. Since the weather now is not only surge and heave, but we can see that the sway is now on par with the surge. Mainly the heave is almost the same. It is also noticeable that the standard deviations of roll, pitch and yaw are also very different than the 0-degree direction.

**X:**

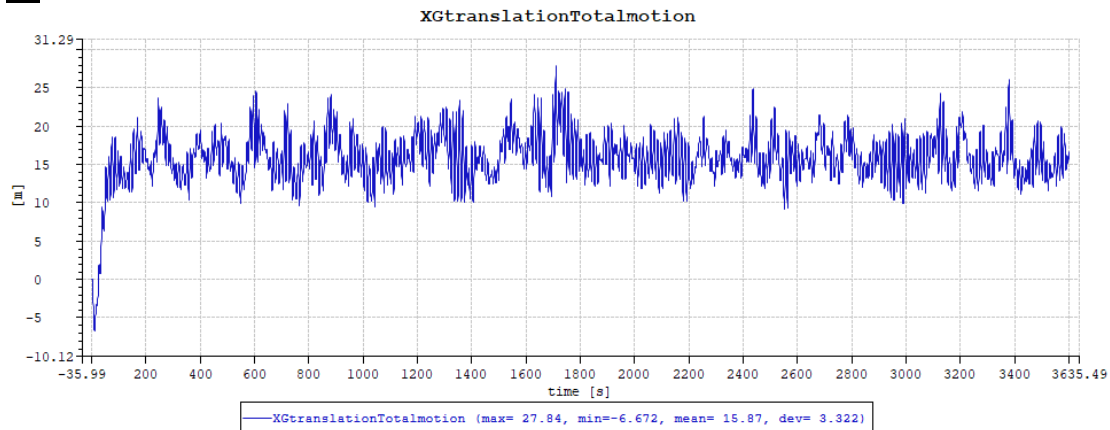


Figure 5.15: Change in X direction 30 Degrees

**Y:**

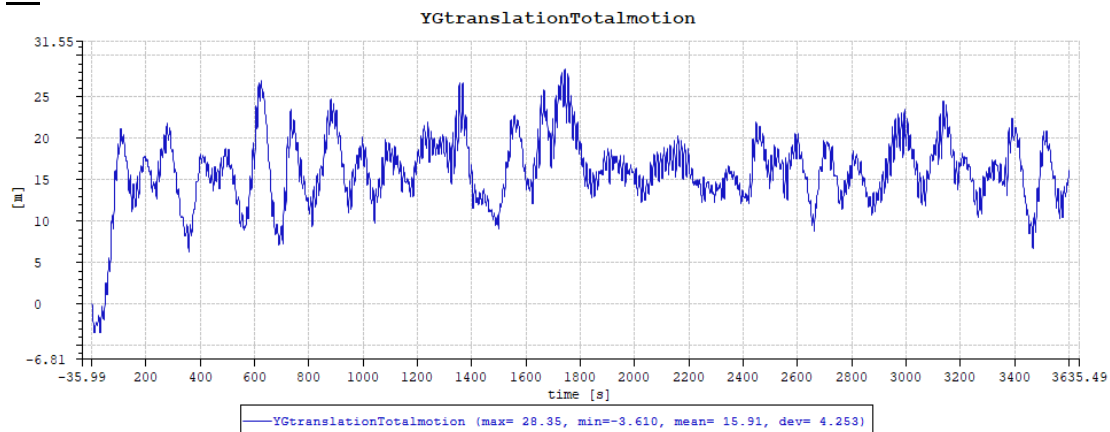


Figure 5.16: Change in Y direction 30 Degrees

**Z:**

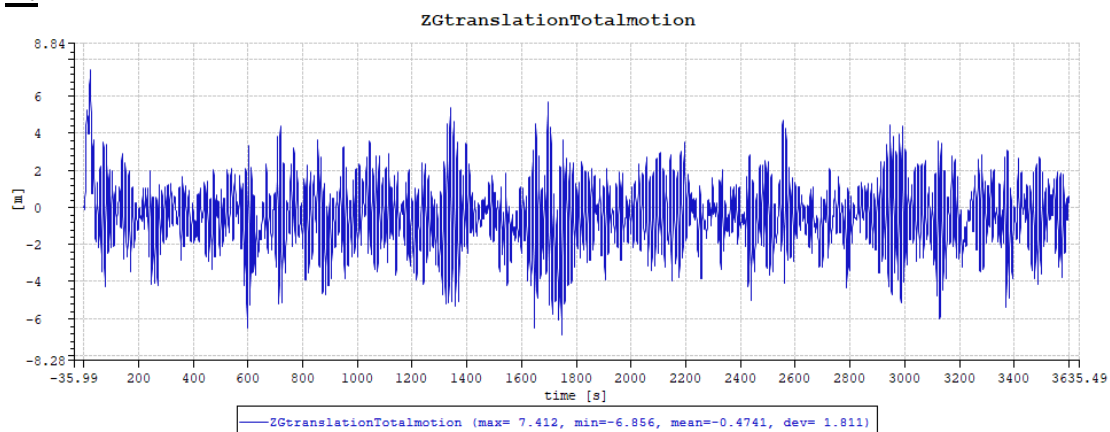
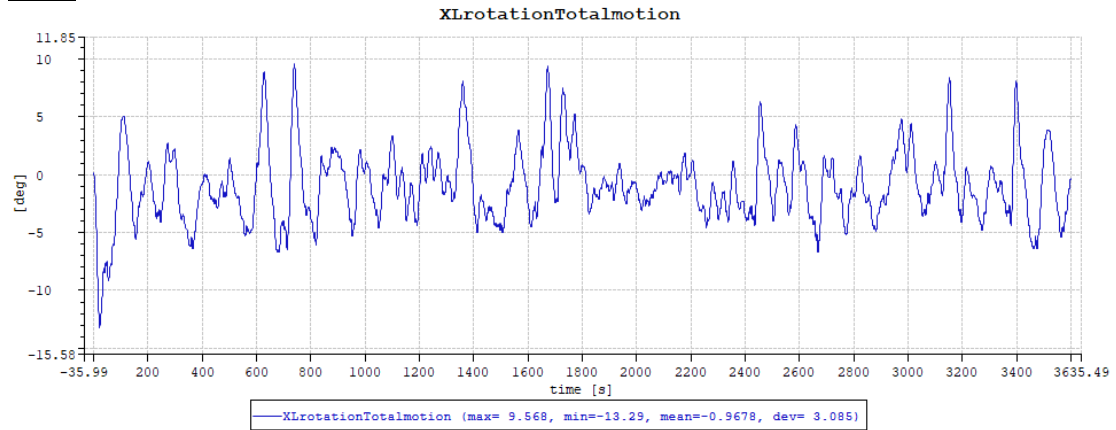


Figure 5.17: Change in Z direction 30 Degrees

### **Roll:**



**Figure 5.18:** Change in Roll 30 Degrees

### **Pitch:**

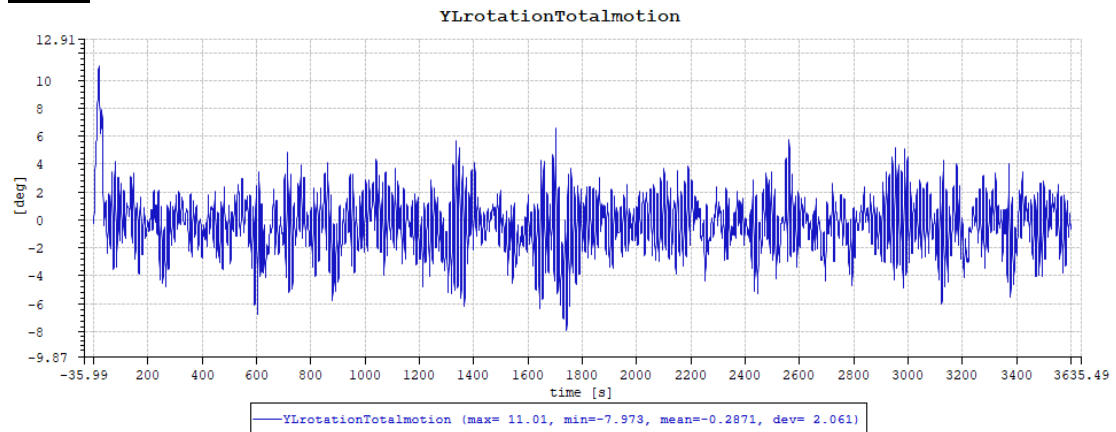


**Figure 5.19:** Change in Pitch 30 Degrees

### **Yaw:**

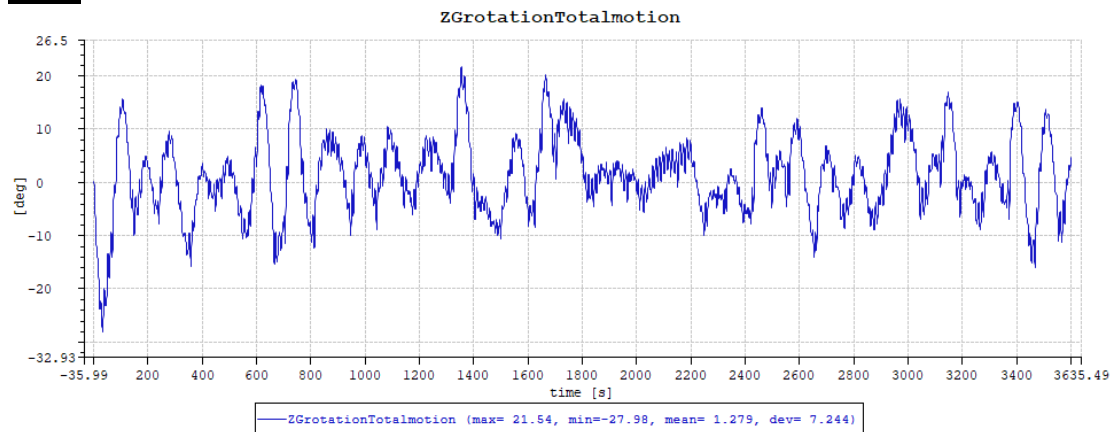


**Figure 5.20:** Change in Yaw 30 Degrees



### 5.3 60 Degree Direction

The 60-degree weather results visit a lesser surge but higher sway than the 30- and 0-degree weather direction results as expected. It is interesting to view a significantly smaller yaw mean compared to the 30-degree direction. Another interesting aspect is the major effect viewed between the 1300 and 1400 second marks. It has had a remarkable impact on the results as all the results show a direct dip or spike in values.

**X:**

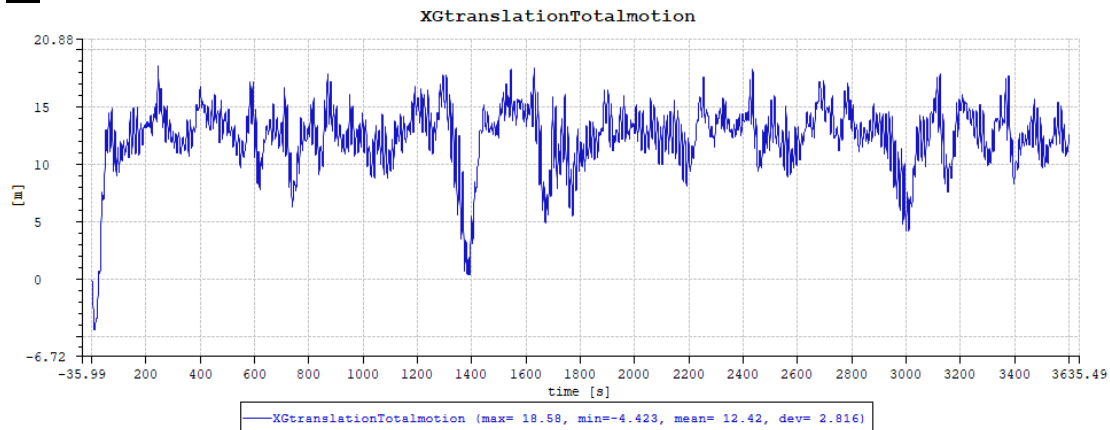


Figure 5.21: Change in X direction 60 Degrees

**Y:**

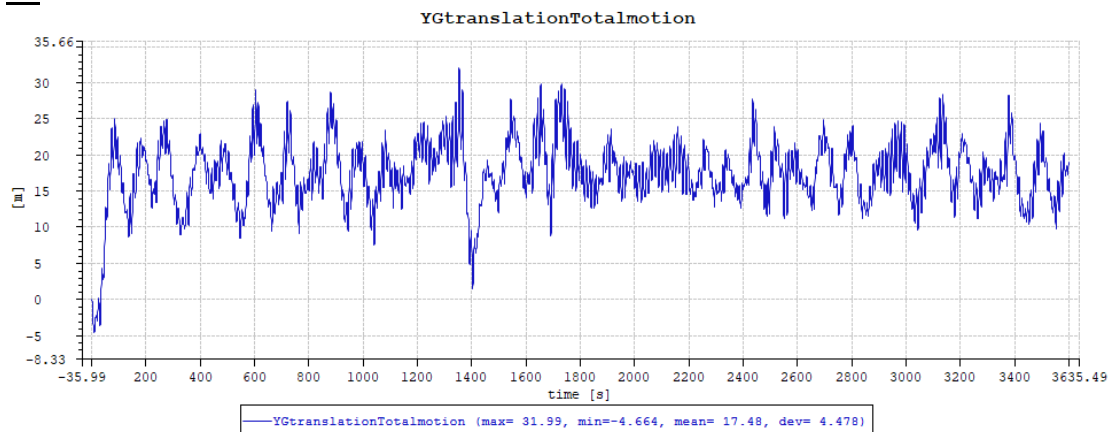


Figure 5.22: Change in Y direction 60 Degrees

**Z:**

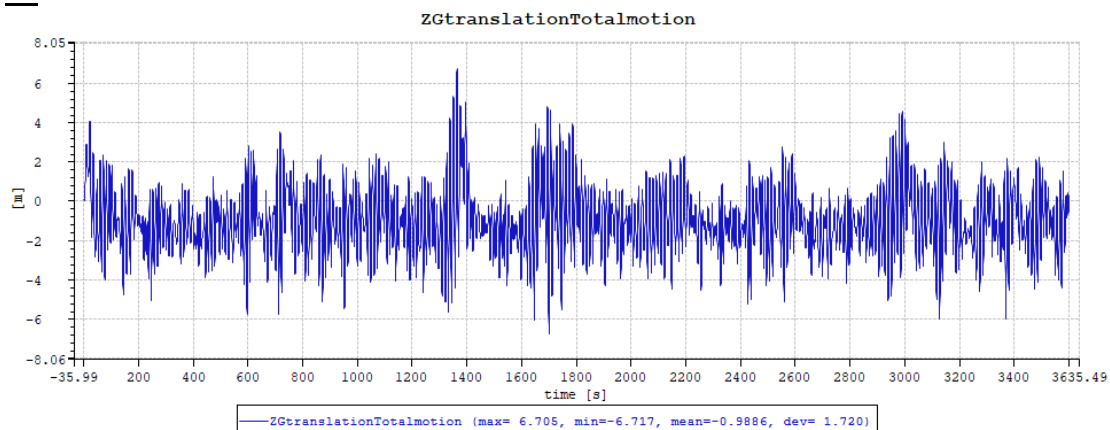


Figure 5.23: Change in Z direction 60 Degrees

### Roll:

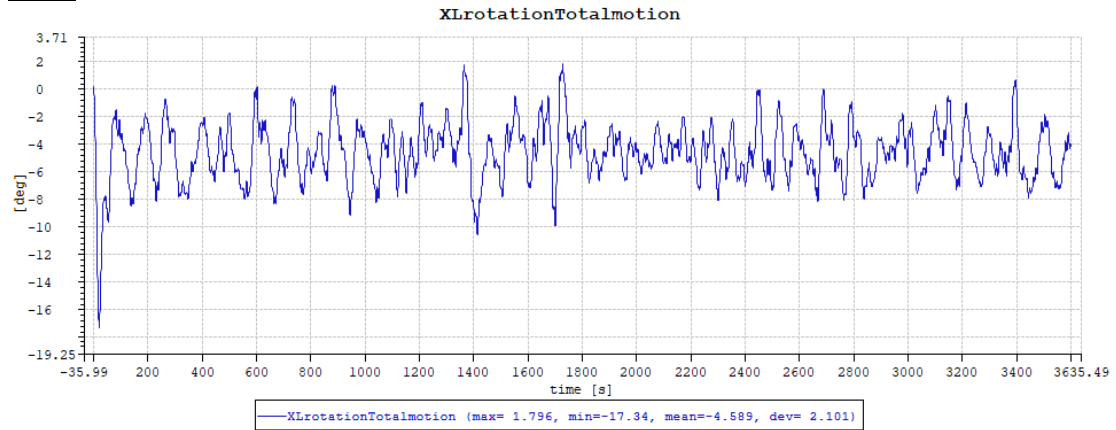


Figure 5.24: Change in Roll 60 Degrees

### Pitch:

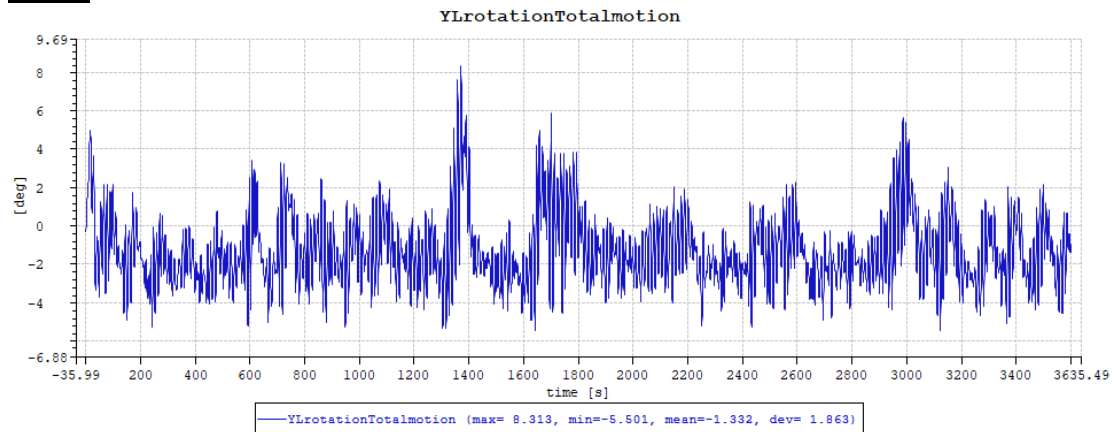


Figure 5.25: Change in Pitch 60 Degrees

### Yaw:

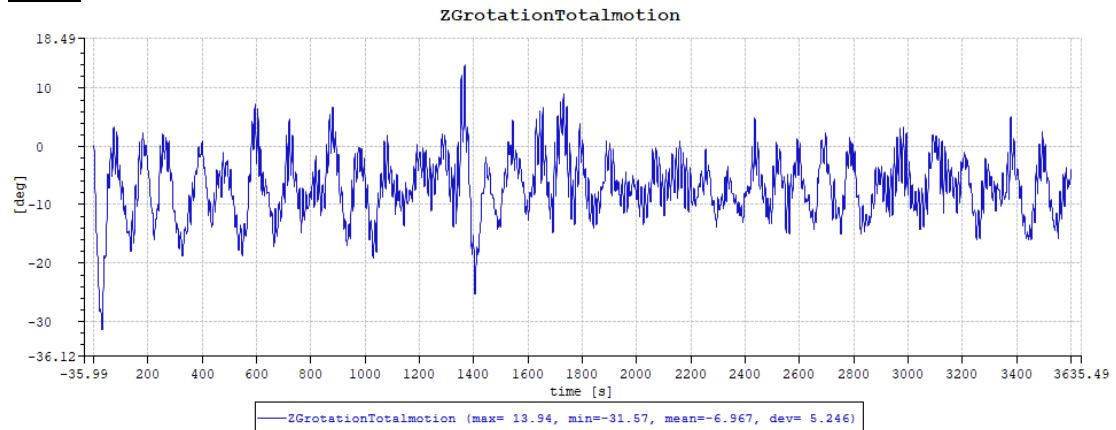


Figure 5.26: Change in Yaw 60 Degrees

From the results shown above, the graphs are congruent with the theory that this thesis is based on.

## 6 Comparison between Sima and Orcaflex

After Sima has produced results in dynamic simulation, the comparison between Orcaflex output and Sima output can be made. There are a few differences that must be taken into consideration when making the comparison between Sima and Orcaflex software:

- Orcaflex uses randomly created wind values for each timestep of the simulation. Sima only uses the mean wind value for the horizontal and vertical wind speeds. This will create a difference in the standard deviations between the results.
- Orcaflex uses a seabed contact specification. The specification is set to Elastic for the catenary system contact point. Sima only checks whether the catenary system either ends on the floor of the sea or if there is contact between the lines and the seabed itself. This is a negligible difference as there aren't many differences in how the whole catenary system reacts to the environment.
- Orcaflex allows for temperature selection of the environment whereas Sima does not use it as a necessary input for the simulation. Again, this is a negligible difference as it doesn't change the output.

The final comparison for the 0-degree weather direction can be seen below:

**Table 6.1:** Comparison of Results in the 0 Degree Weather Direction

<b>0 Degree Weather Direction</b>	<b>Orcaflex</b>	<b>Sima</b>
<b>X mean</b>	14,48	14,86
<b>Y mean</b>	0,6	0,03
<b>Z mean</b>	-0,32	-0,032
<b>Roll mean</b>	0,31	0,037
<b>Pitch mean</b>	0,68	0,33
<b>Yaw mean</b>	0,27	0,41
<b>X std</b>	3,27	3,65
<b>Y std</b>	0,08	0,08
<b>Z std</b>	1,74	1,83
<b>Roll std</b>	0,04	0,02
<b>Pitch std</b>	2,16	2,13
<b>Yaw std</b>	0,27	0,10

As can be seen in the table, the values that have been reported are very close to each other. The major differences seem to be in the standard deviation part of the table which has been related to the difference in wind input type. Before making a conclusion, however, the other weather direction results must also be taken into consideration

The final comparison for the 30-degree weather direction can be seen below:

**Table 6.2:** Comparison of Results in the 30 Degree Weather Direction

<b>30 Degree Weather Direction</b>	<b>Orcaflex</b>	<b>Sima</b>
<b>X mean</b>	15,29	15,87
<b>Y mean</b>	16,81	15,91
<b>Z mean</b>	-0,58	-0,47
<b>Roll mean</b>	-0,23	-0,96
<b>Pitch mean</b>	0,01	-0,28
<b>Yaw mean</b>	-7,09	1,28
<b>X std</b>	2,48	3,32
<b>Y std</b>	2,14	4,25
<b>Z std</b>	1,23	1,81
<b>Roll std</b>	1,72	3,08
<b>Pitch std</b>	1,76	2,06
<b>Yaw std</b>	2,12	7,24

The differences start to grow to bigger extents as the weather direction increases. The major divide is evident in the difference between Yaw mean and Yaw std. The other values save for a small difference in standard deviation, are relevant to each other. What is interesting is that the Orcaflex simulation reports a negative Yaw while Sima reports a positive yaw. To understand this better, a higher wind direction is needed.

The final comparison for the 60-degree weather direction can be seen below:

**Table 6.3:** Comparison of Results in the 60 Degree Weather Direction

<b>60 Degree Weather Direction</b>	<b>Orcaflex</b>	<b>Sima</b>
<b>X mean</b>	12,5	12,42
<b>Y mean</b>	21,58	17,48
<b>Z mean</b>	-0,7	-0,9
<b>Roll mean</b>	-0,18	-4,59
<b>Pitch mean</b>	-0,42	-1,33
<b>Yaw mean</b>	-8,93	-6,97
<b>X std</b>	1,79	2,82
<b>Y std</b>	3,28	4,48
<b>Z std</b>	1,27	1,72
<b>Roll std</b>	2,37	2,10
<b>Pitch std</b>	1,18	1,86
<b>Yaw std</b>	2,48	5,25

The difference between the Yaw means and the Yaw standard deviation has decreased, however the difference in Roll mean starts to grow. This result is further investigated.

The major differences between the results have been traced to firstly the wind data input and the hub placement. How the hub is placed on the top of the tower in Orcaflex is by denoting the slender system connection. To “lock” the hub on the Simo tower needs docking cones. These docking cones which are presented in the example wind turbine

can't be changed in direction. Thus, as the weather direction changes, the hub behavior starts to change rapidly as well. The Orcaflex model has a rotating hub which faces the direction of the weather at every different angle whereas the Simo model can only point towards the 0-degree direction which creates a major difference.

## 7 Conclusion and Future Work

From setting up the models to receiving the results, the Sesam package allows for an integrated series of modules to perform a strong analysis. The objective of this thesis was to be able to perform a dynamic analysis on a FOWT, with the analysis performed, the results have also been compared to that of Orcaflex. With some differences in inputs having major effects on the results, it is good to see the results are coinciding more than not. The Sesam modules are intuitive and have many documentations available for support of the user. It is entirely possible to use the Sesam package to start from scratch and run a dynamic analysis. Furthermore, the Sesam package also allows for calculations of specific parts of the vessel.

One of the discussed goals for this thesis was to compare the regression analysis method to that of the FEA method in Sesam package. The methodology is further investigated in “A regression and beam theory-based approach for fatigue assessment of containership structures including bending and torsion contributions” (Mao, et al., 2015). This method could have been compared if it was possible to get the sectional loads from a Wasim application in Sesam. However, due to version differences it was possible to run a Wasim analysis.

As part of further work, the exporting of Sima results to Wasim could be done. This is a possibility with Sima software that enables a package of data which can be used in Wasim as an input to be able to run the analysis. However, this was not done in this project as the Wasim application could only be found on an older version of Hydro-D with little documentation. Thus, it would require more investigation so that the data could be transferred to the analysis. Theoretically the Wasim application should be able to provide the sectional loads which are required to compare the FEA method and the method the journal suggests. This would also require more simulations to be run on Sima to make sure the exported data is valid.

Another note to be made is that with the current Sima values, the differences are mainly due to the wind input and the docking cone problem. With further investigation, the data could be re-generated within the Turbosim application in Sima and input to reduce the difference. The problem with the docking cones will still take manhours to complete as the required data for the thrust to be modified is still an issue. With even more time, the actual 10MW tower could be put in the Sima analysis to be able to get the most accurate results.

The time limit of 3600 seconds could also be increased to view a longer span of time.

The installjac package also can be used to simulate the actual installation of the vessel to see if the vessel works according to the required specifications. The docking cone problem is present here as well as the tension and thrust in the nacelle creates unreliable data which can't be used in understanding the exact behavior of the RNA.

The current setup works for extreme storm conditions, with more time, the behavior for less than 25 m/s, above 5 m/s windspeed could be tested. This would also view the moment created by the turning of the actual blades of the turbine. The turbine thrust can also be added to the analysis.

## 8 References

- Beji, S., 2020. Formulation of wave and current forces acting on a body and resistance of ships. *Ocean Engineering*, Volume 218.
- Beshbichi, O. E., Xing, Y. & Ong, M. C., 2021. An object-oriented method for fully coupled analysis of floating offshore wind turbines through mapping of aerodynamical coefficients. *Marine Structures*, Volume 78.
- Bi, Z., 2019. Solutions of Element Models. In: *Finite Element Analysis Applications*. s.l.:s.n.
- Byju's, 2022. *Fourier Transform*. [Online]  
Available at: <https://byjus.com/maths/fourier-transform/>
- Constantin, P. & Ciprian, F., 1989. *Navier-stokes equations*. Chicago: Univ. Chicago Pr..
- DNV, 2022. *Sesam Feature Description*. s.l.:DNV.
- DNV, 2022. *Simo Documentation*. [Online]  
Available at: [https://www.simo-project.org/documentation/SIMO\\_manual.pdf](https://www.simo-project.org/documentation/SIMO_manual.pdf)  
[Accessed 2022].
- DNV, 2022. *Sintef: Motion Transfer Functions*. [Online]  
Available at: [https://www.sima.sintef.no/riflex/theory/motion\\_transfer\\_functions.thml](https://www.sima.sintef.no/riflex/theory/motion_transfer_functions.thml)
- DNVGL, 2022. *DNVGL Hydro-D User Manual HydroD V6.0.0 Docs*. [Online].
- DNVGL, 2022. *GeniE User Documentation - GeniE V8.3-04 User Documentation*. [Online]  
Available at: <https://myworkspace.dnv.com/download/sesam/user-manual/genie-8-3-04/UserDocumentation.html>
- el Moctar, O., Lantermann, U. & Chilcice, G., 2022. An efficient and accurate approach for zero-frequency added mass for maneuvering simulations in deep and shallow water. *Applied Ocean Research*.
- Hermenau, R., 2013. *Pitch-sway-yaw-heave*. [Online]  
Available at: <https://www.xsimulator.net/simtools-quickstart/pitch-sway-yaw-heave/>
- Jonkman, J., 2010. Definition of the Floating System for Phase IV of OC3.
- Kristiansen, E. & Egeland, O., 2003. Frequency-Dependent Added Mass in Models for Controller Design for Wave Motion Damping. *IFAC Proceedings*, 36(21), pp. 67-72.
- Larsen, T. J. & Hansen, A. M., 2015. *How 2 HAWC2, the user's manual*. Roskilde: Technical University of Denmark.
- Li, L., 2022. Full-coupled analysis of offshore floating wind turbine supported by very large floating structure with consideration of hydroelasticity. Volume 189, pp. 790-799.
- Mansur, W., Soares, D. & Ferro, M., 2004. Initial conditions in frequency-domain analysis: the FEM applied to the scalar wave equation. *Journal of Sound and Vibration*, 270(4-5), pp. 767-780.
- Mao, W., Li, Z., Ogeman, V. & Ringsberg, J., 2015. A regression and beam theory based approach for fatigue assessment of containership structures including bending and torsion contributions. *Marine Structures*, Volume 41, pp. 244-266.
- Meysam, K., Hall, M., Buckham, B. & Crawford, C., 2017. A multi-objectivedesign optimization approach for floating offshore wind turbine support structures. *Journal of Ocean Engineering and Marine Energy*, Volume 3, pp. 1-19.
- Morison, J., Johnson, J. & Schaaf, S., 1950. The forces exerted by surface waves on piles. *Petroleum Trans*.

Ojo, A., Collu, M. & Coraddu, A., 2022. Multidisciplinary design analysis and optimization of floating offshore wind turbine substructures: A review. *Ocean Engineering*, Volume 266, p. Part 1.

Orcina, 2022. *Morison's equation*. [Online]  
Available at:  
<https://www.orcina.com/webhelp/OrcaFlex/Content/html/Morison%27sequation.html>

Orcina, 2022. *Vessel theory: Impulse response and convolution*. [Online]  
Available at:  
<https://www.orcina.com/webhelp/OrcaFlex/Content/html/Vesseltheory,Impluseresponseandconvolution.htm>

Orcina, 2022. *Vessel types: Stiffness, added mass and damping*. [Online]  
Available at:  
<https://www.orcina.com/webhelp/OrcaFlex/Content/html/Vesseltypes,Stiffness,addedmassandddamping.html>

Pascual, B. & Adhikari, 2008. *Dynamic Response of Structures with Frequency Dependent Damping*. [Online]  
Available at: [engweb.swan.ac.uk/~adhikaris](http://engweb.swan.ac.uk/~adhikaris)

Pegalajar-Jurado, A., Borg, M. & Bredmose, H., 2022. An efficient frequency-domain model for quick load analysis of floating offshore wind turbines.. *Wind Energy Science*, Volume 3, pp. 693-712.

Pillai, A. et al., 2022. Anchor loads for shallow water mooring of a 15 MW floating wind turbine-Part II: Synthetic and novel mooring systems. *Ocean Engineering*, Volume 266.

Seo, M.-G., Park, D.-M., Yang, K.-K. & Kim, Y., 2013. Comparative study on computation of ship added resistance in waves. *Ocean Engineering*, Volume 73, pp. 1-15.

Sethuraman, L. & Venugopal, V., 2013. Hydrodynamic response of a stepped-spar floating wind turbine: Numerical modelling and tank testing. *Renewable Energy*, Volume 52, pp. 160-174.

Sintef, 2022. *SIMO 4.20.4 Theory Manual*, s.l.: Sintef.

Song, Y. et al., 2021. Dynamic reliability analysis of a floating offshore wind turbine under wind-wave joint excitations via probability density evolution method. *Renewable Energy*, Volume 168, pp. 991-1014.

ToolBox, E., 2022. *Mass Moment of Inertia*. [Online]  
Available at: [https://www.engineeringtoolbox.com/moment-inertia-torque-d\\_913.html](https://www.engineeringtoolbox.com/moment-inertia-torque-d_913.html)

Ullah, Z., Muhammad, N. & Choi, D.-H., 2021. On the importance of nonlinear hydrostatic stiffness of offshore floating wind turbine platforms. *Applied Ocean Research*, Volume 113.

USCG, 2022. *Operations home*. [Online]  
Available at: <https://www.dco.uscg.mil/OCSNCOE/MODU/Types-of-MODUs/>

Wandji, W. N., Natarajan, A. & Dimitrov, N., 2016. Development and design of a semi-floater substructure for multi-megawatt wind turbines at 50+m water depths. *Ocean Engineering*, pp. 226-237.

Wang, B. et al., 2022. Motion characteristics and aero-elastic responses of floating offshore wind turbine under coupling action of waves and winds. *Frontiers in Environmental Science*, August. Volume 10.

Wang, Y., Tang, Z., Wang, L. & Wang, X., 2021. Linear and quadratic damping coefficients of a single module of a very large floating structure over variable bathymetry: Physical and numerical free-decay experiments. *Journal of Ocean Engineering and Science*.



Yang, Y. et al., 2020. Wind-wave coupling effects on the fatigue damage of tendons for a 10MW multi-body floating wind turbine. *Ocean Engineering*, Volume 217.

## 9 Appendix A: Software Images

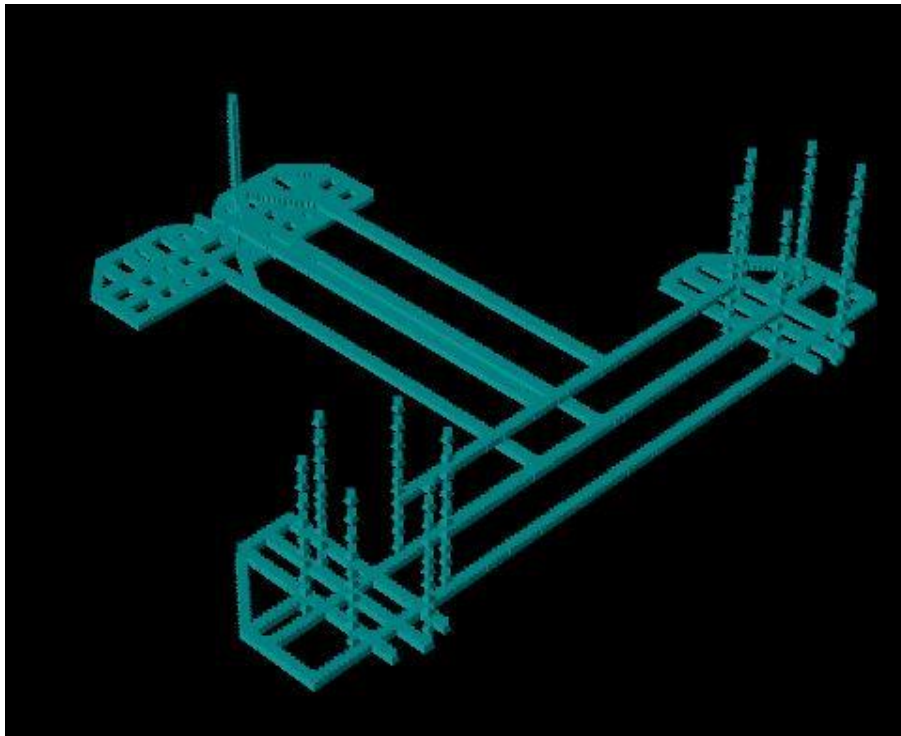


Figure 9.1: T1 model in GeniE

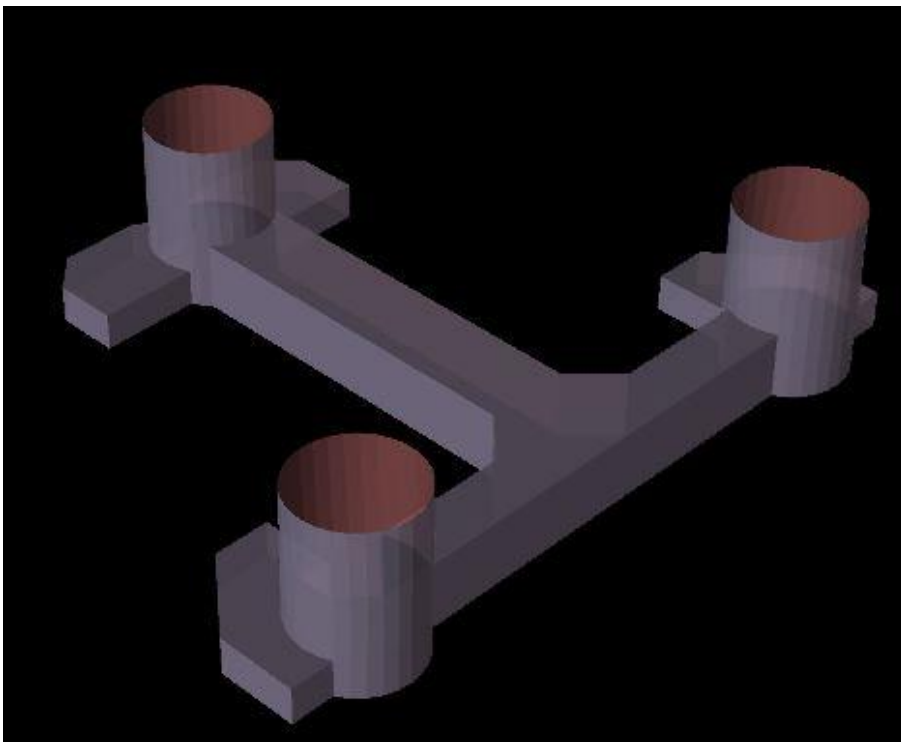
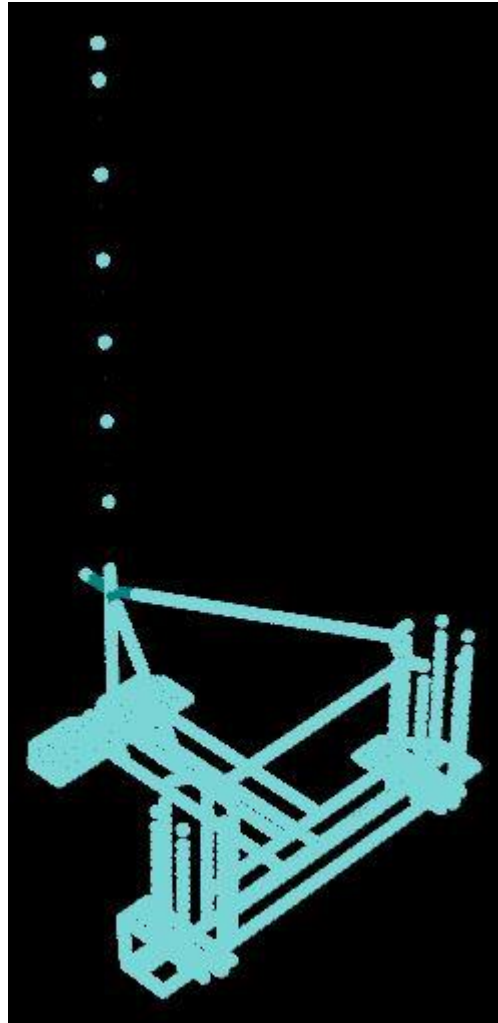
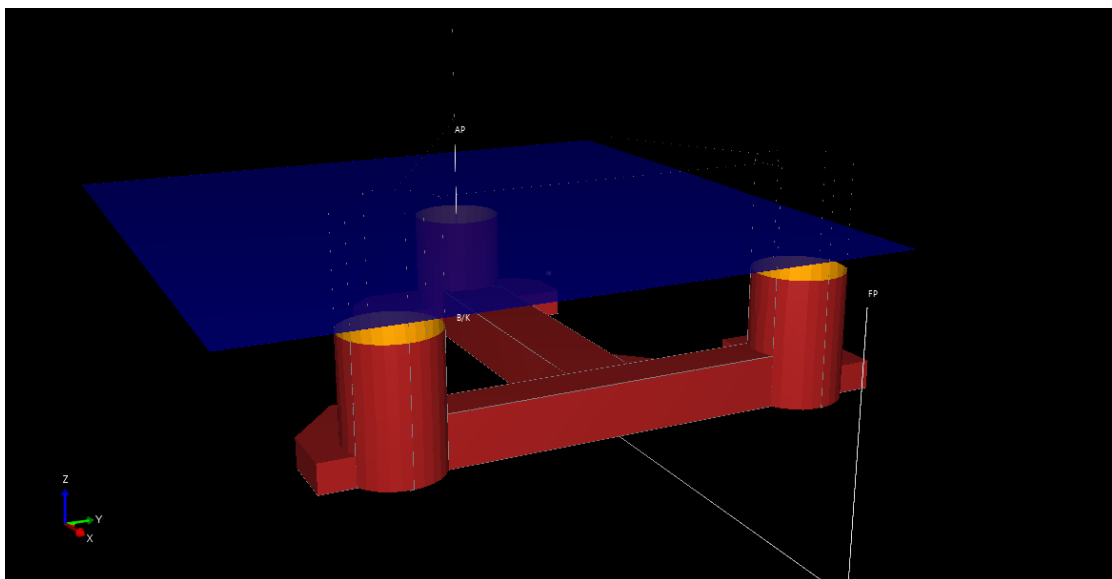


Figure 9.2: T2 model in GeniE



**Figure 9.3:** T5 model in GeniE



**Figure 9.4:** Hydro-D Model Composite

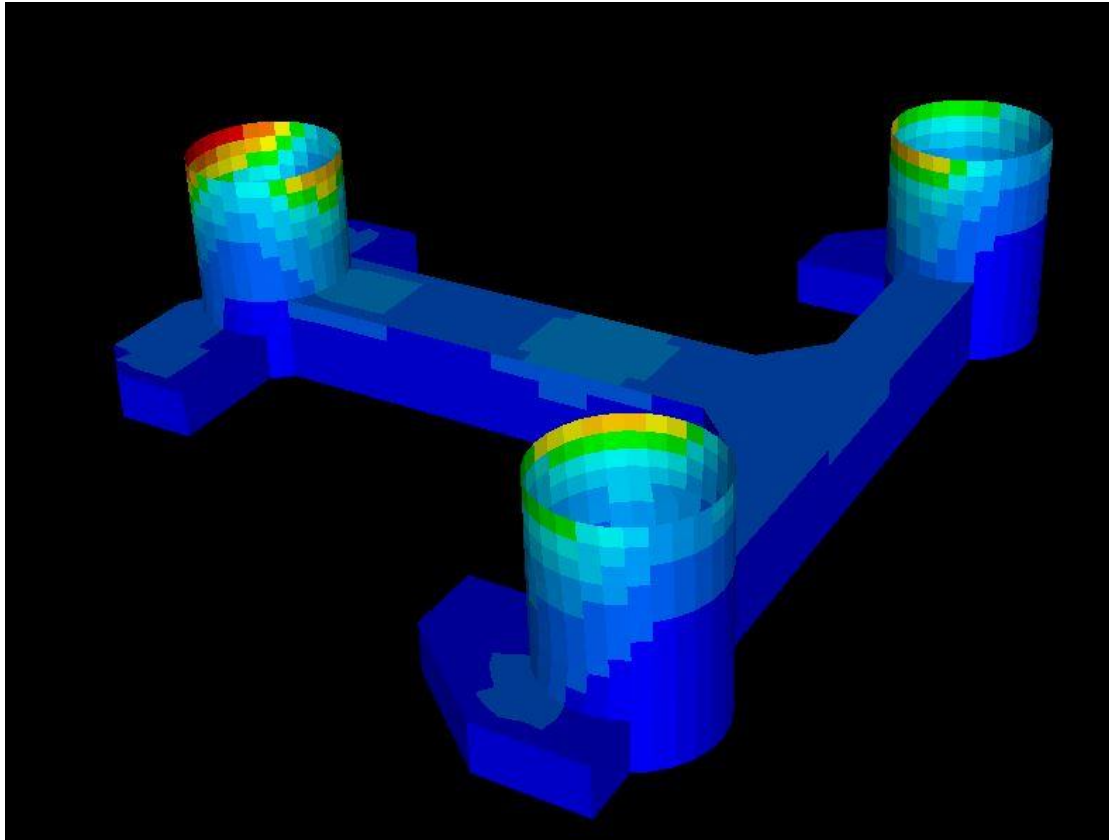


Figure 9.5: Xtract Pressure view from 0 Deg Weather Direction

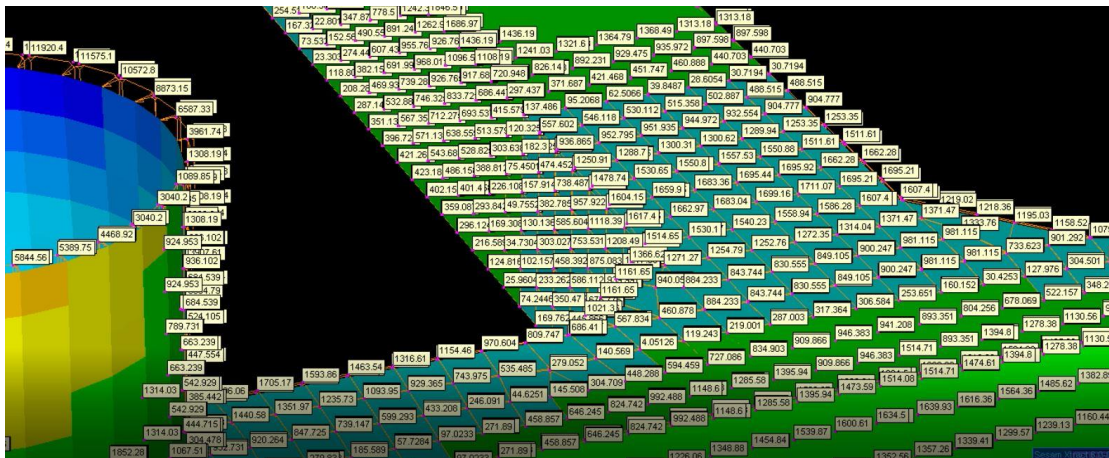
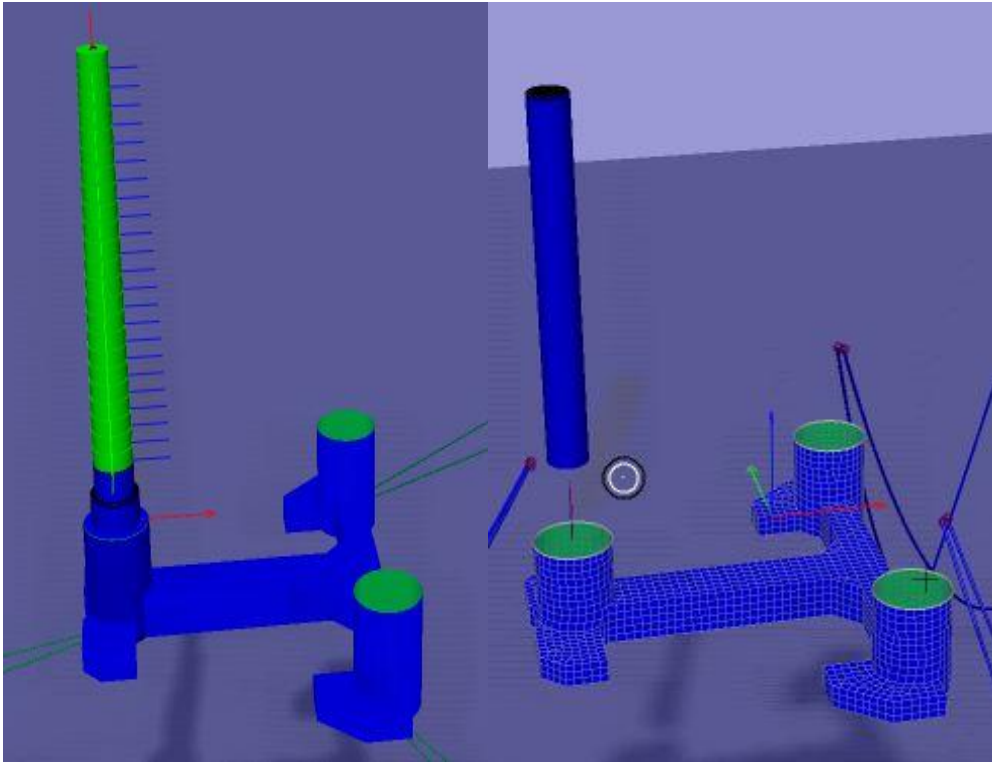
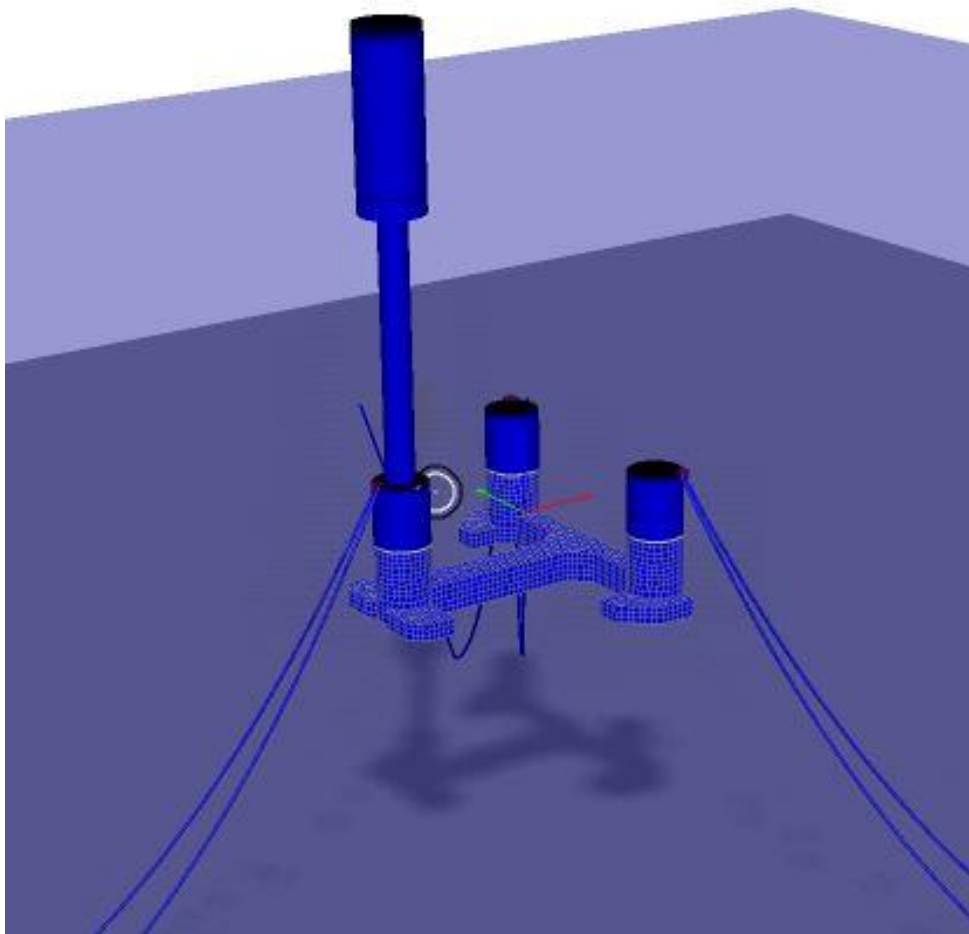


Figure 9.6: Wadam Analysis Pressure Distribution



**Figure 9.7:** Riflex Tower (left) and Simo Tower (right).



**Figure 9.8:** Sima Cylinder RNA

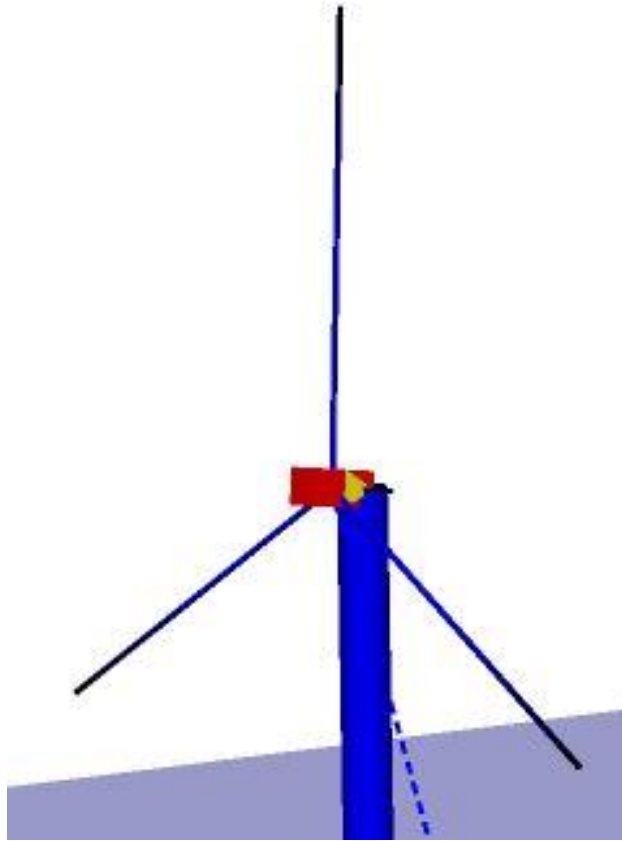


**Figure 9.9:** Simo Hub



**CHALMERS**  
UNIVERSITY OF TECHNOLOGY